Stony Brook University

Modulation of Rodent Central Respiratory Network Dynamics

and Respiratory Phase Interactions

A Dissertation Presented

by

Tabitha Yun-Ching Shen

to

The Graduate School

in Partial Fulfillment of the

Requirements

for the Degree of

Doctor of Philosophy

in

Biomedical Engineering

Stony Brook University

December 2014

Stony Brook University

The Graduate School

Tabitha Yun-Ching Shen

We, the dissertation committee for the above candidate for the
Doctor of Philosophy degree, hereby recommend
acceptance of this dissertation.

Irene C. Solomon
Professor, Physiology and Biophysics

Emilia Entcheva
Professor, Biomedical Engineering

Leon Moore
Professor, Physiology and Biophysics

William F. Collins
Associate Professor, Neurobiology and Behavior

Brendan J. Canning
Associate Professor, Division of Allergy and Clinical Immunology, Johns Hopkins University

This dissertation is accepted by the Graduate School

Charles Taber
Dean of the Graduate School

Abstract of the Dissertation

Modulation of Rodent Central Respiratory Network Dynamics

and Respiratory Phase Interactions

by

Tabitha Y. Shen

Doctor of Philosophy

in

Biomedical Engineering

Stony Brook University

2014

Modulation of the central neural control system governing breathing is a critical mechanism for maintaining homeostasis of a functioning physiological system. Perturbations can be either endogenous or exogenous to the respiratory control system, meaning there are factors that modulate the respiratory control centers either directly (endogenously) or indirectly via feedback mechanisms (exogenously). We hypothesized that perturbations to the neural controller would cause changes in the configuration of the neural network, as evidenced by changes in slow and fast oscillatory respiratory network dynamics. To test this hypothesis, we use both an *in vitro* and an *in vivo* rat experimental preparation in conjunction with perturbations to disrupt homeostasis endogenously and exogenously. In the *in vitro* preparation, we perturbed the respiratory system endogenously by changing either the temperature or the K^+ concentration of the artificial cerebral spinal fluid. In the *in vivo* preparation, we perturbed the system exogenously by eliciting sneeze or micturition reflexes. We analyzed neurogram and/or electromyogram activity data from multiple respiratory-related outputs to characterize and quantify timing, patterning, and phase-related variability between respiratory outputs in order to gain insight on how the brainstem is reorganized to intrinsically modulate control of the diaphragm and upper airways. Both endogenous and exogenous perturbations altered the neural network resulting in modulation of various aspects of respiratory-related discharge. Endogenous perturbations modified the respiratory network components that govern respiratory burst generation and the relationship between respiratory outputs, but respiratory rhythm was uninterrupted. Moreover, endogenously-mediated changes in excitability produced same direction changes in the synchrony or

orderliness of the network. In contrast, exogenous perturbations modified respiratory network components that generate respiratory rhythm resulting in a disruption of fundamental underlying respiratory behavior, which was evident by the production of dysrhythmia and altered phase-timing between different respiratory-related outputs. In conclusion, the respiratory network is dynamic on a breath-to-breath basis and reconfigures to maintain a functional physiological system.

Dedication Page

This body of work is dedicated to the many people who have mentored and guided me through this process.

Table of Contents

List of Figures

List of Tables

List of Abbreviations

$[K^+]_o$	Extracellular potassium concentration
ABD	Abdominal nerve
aCSF	Artificial cerebral spinal fluid
CPG	Central pattern generator
Dia	Diaphragm
E	Expiration
EMG	Electromyography
EO	External oblique
EUS	External urethral sphincter
HFO	High frequency oscillation
HT	High temperature
I	Inspiration
ICI	Intercontraction interval
LT	Low temperature
LUT	Lower urinary tract
MFO	Medium frequency oscillation
nPhr	Number of experiments with phrenic recordings
nXII	Number of experiments with XII recordings
$PaCO_2$	Arterial partial pressure of carbon dioxide
PAG	Periaqueductal gray
PaO_2	Arterial partial pressure of oxygen
Phr	Phrenic nerve
Pre-I	Pre-Inspiratory respiratory phase
PSD	Power spectral density
RLN	Recurrent laryngeal nerve
T	Tongue
TE	Expiratory duration
TF	Time frequency
T_I	Inspiratory duration
T_I/T_{Total}	Inspiratory duty cycle
T_{total}	Duration of 1 breath
XII	Hypoglossal nerve
XII_P	Pre-Inspiratory portion of XII nerve activity
XII_{P+I}	Full XII nerve activity (pre-I and I phases)

Acknowledgments

I would like to thank my committee members, in particular Dr. Solomon and Dr. Collins, for investing in my academic maturity and development. I would like to thank Dr. Inefta Reid-Martin and Dr. Kenichi Ono for working with me and encouraging me to be excellent in technical and critical skills

Chapter 1: Introduction

Background and Significance

Homeostasis is necessary for maintaining function in mammals. The body must have processes to sense and adapt to different perturbations, which might be endogenous or exogenous. The respiratory system is a network of neurons designed to adapt to many states. It is one of the systems responsible for maintaining key homeostatic levels such as arterial blood gasses (PaO_2 and $PaCO_2$) and autonomic nervous system balance (*i.e.*, blood pressure, heart rate, etc.) which all are key to maintaining an environment suitable for a functioning biological system.

Respiratory activity in mammals is known to be generated and modulated by a network of neurons in the dorsolateral pontine respiratory group and medullary ventrolateral respiratory column (Smith, Abdala, Koizumi, Rybak, & Paton, 2007; St-John, 1998; St John, 1985; G. Stella, 1938). Additionally, other areas of the midbrain, such as the periaqueductal grey, have been shown to contribute to respiratory rhythm maintenance (Holstege, 2013). The area of the brainstem essential to respiratory rhythm generation is in the lower brainstem (Lumsden, 1923) and has been identified as the pre-Bötzinger complex (pBC) (Rekling & Feldman, 1998; Smith, Ellenberger, Ballanyi, Richter, & Feldman, 1991). To understand the control mechanisms of the network that controls breathing, we can analyze signals from the neural output that controls the pump muscles and airway resistance, which ultimately create the breathing behavior.

Temporal and spectral-domain dynamics have been used to characterize neural output recorded from respiratory related nerves. Parameters such as breathing frequency, inspiratory duration (T_I), expiratory duration (T_E), inspiratory duty cycle (T_I/T_{Total}), are used to give an idea of gross changes in respiratory drive or activity. However, because these nerves are a

compilation of multiple modulators, it is not readily apparent as to what is happening to the neural network and/or how it is changing due to perturbations. Therefore, analysis in the spectral and information domain may provide more insight into network dynamics by increasing understanding of the fast-oscillatory rhythms within each neural burst.

Previous experiments in multiple animal models have shown that, when analyzed with a power spectral density (PSD) estimation, fast-oscillatory respiratory rhythms within these neural bursts exhibit characteristic peak frequencies in 2 ranges: a medium frequency oscillation (MFO) between 40-50 Hz (Cohen, See, Christakos, & Sica, 1987; Richardson & Mitchell, 1982) and a high frequency oscillation (HFO) between 90-110 Hz (Cohen et al., 1987). An additional higher frequency (ultra high frequency oscillation; UHFO) at 130-150 Hz was also reported in a mouse model (O'Neal, Spiegel, Chon, & Solomon, 2005). It has been suggested that HFO activity is related to medullary or pontine inspiratory neuron activities while MFO activity is correlated with respiratory motoneuron activities (Cohen, Piercey, Gootman, & Wolotsky, 1974; Funk & Parkis, 2002). Because the two peaks perhaps arise from different control centers, the power (amplitude) of the peak frequencies can give insight into how much either is contributing to the network. However, because the respiratory system is a highly dynamic system, a time-invariant spectral analysis may not be appropriate since those methods assume a stationary process. Time-varying analysis techniques such as short-time Fourier transforms, wavelet analysis or a smoothed-pseudo Wigner-Ville distribution (SPWD), can be used to estimate the timing of frequency dynamics over time. The SPWD method provides a few advantages over the other methods, namely its uniform resolution across time and frequency, and better time and frequency resolution because the signal is not segmented into small segments, and therefore this was the chosen method of time-frequency (TF) analysis.

Another strategy of gaining insight into the intrinsic network dynamics is to use a nonlinear dynamical analysis of neural output in the complexity domain, which gives insight into how complex a signal is. One such method is approximate entropy (ApEn) (Pincus & Huang, 1992), which provides a statistical index of regularity (orderliness) of a signal in the time domain. This method can be used as an indicator of the number of components in the network generating the signal and help quantify how these components are changing. While there other methods exist that provide insight into the information domain (e.g., sample entropy and fuzzy entropy), we have found that ApEn is the most appropriate to date for fast neurophysiological signals (Chen, Solomon, & Chon, 2004).

Many anatomically distinct groups of neurons that contribute to the generation of respiration, which enables the respiratory network to produce multiple patterns of respiratory output. These groups include areas responsible for central chemoreception, afferent signal processing, rhythm generation and motor pattern formation. There are a multitude of breathing patterns and breath types, including apneusis, augmented breaths, hyper- and hypoventilation, but for this project we will focus on eupnea and gasping.

Eupnea is defined as normal, unconscious breathing. While the definition of eupnea varies between species, there are some characteristics that are conserved. Eupneic breathing can be broken up into 3 phases: inspiration, post-inspiration and expiration (Richter, 1982; Richter, Ballantyne, & Remmers, 1986; Smith et al., 2007; St-John, 1998; St John, 1985; G. Stella, 1938). Inspiration generally is defined based on diaphragm or phrenic nerve activity, and the quiescent periods are defined as expiration. Pre-inspiratory activity occurs during the end of the expiratory phase but is activity associated with inspiratory related outputs (e.g., hypoglossal nerve output or

tongue electromyography (EMG) activity). For instance, the hypoglossal nerve has neural activity prior to inspiration, as defined by the onset of phrenic nerve activity, that is associated with the opening of the airways.

Nerves associated with the respiratory network that will be discussed here are the phrenic nerve, the hypoglossal nerve (a.k.a. cranial nerve XII), the recurrent laryngeal (RLN) and the abdominal nerve (ABD). The phrenic nerve, which when activated defines the inspiratory phase, exits the spinal column at C3-C5 and is the sole nerve which innervates the diaphragm. The XII nerve branches into two; the medial branch (associated with tongue protrusion), and the lateral branch (associated with tongue retrusion). Unlike phrenic nerve activity, during eupnea, XII nerve activity is present during both pre-inspiratory (preI) and inspiratory (I) respiratory phases. The RLN is a branch of the Vagus nerve responsible for innervating all the intrinsic muscles of the larynx except for the cricothyroid muscles. RLN activity spans both inspiratory and expiratory phases but pauses at the end of phrenic activity and restarts in the early expiratory phase. The ABD has many branches, all of which only show neural activity during active expiration or reflexes such as sneezing and coughing.

There are two classes of perturbations that can disrupt homeostasis controlled by the respiratory network: endogenous and exogenous. Endogenous perturbations can be defined as conditions that change the excitability of neurons that control breathing by altering their intrinsic properties; and exogenous perturbations can be defined as conditions that change the excitability of neurons that control breathing by reflex/afferent input. There are many perturbations that can disrupt homeostasis, but for the purpose of this project we will focus on two endogenous perturbations, a change in temperature and extracellular K^+, and an exogenous perturbation, the effects of the micturition reflex on respiration.

Preparations that are used to study respiratory behavior often are reduced preparations. These reduced preparations, such as the en bloc preparation or transverse medullary slice preparation, often are studied at non-physiological conditions. To decrease degradation of the tissue, metabolism is decreased by maintaining the tissue at lower temperatures (as low as 28°C), and to compensate for the decrease in metabolism, which affects the breathing frequency, elevated extracellular K^+ (which range from mostly range between 4.25 and 9 mM $[K^+]_o$) levels often are used. In order to understand findings from these different preparations it is important to understand how changing temperature and $[K^+]_o$ alter intrinsic properties of the network that generates breathing.

Elevating $[K^+]_o$ and temperature have similar affects in the temporal domain in that they both increase breathing frequency, and yet the network by which the respiratory network is modulated is different. In reduced preparations, increased K^+ increases the network excitability, as evidenced by fictive breathing frequency (Okada, Kuwana, Kawai, Mückenhoff, & Scheid, 2005). Although not statistically significant, trends of increased drive (e.g., decreased T_I, increased respiratory rate and a decreased time-to-peak) were seen as $[K^+]_o$ increased (St John, 1985). In addition to understanding the effects of elevating $[K^+]_o$ studying the effects of elevated $[K^+]_o$ has physiological relevance. For instance, it is known that cerebral spinal fluid and plasma K^+ levels differ, there are a variety of disorders that exhibit electrolyte imbalances, anoxic and ischemic conditions will alter $[K^+]_o$ on the surface of the brain cortex (Hansen, 2008a, 2008b).

Because ion kinetics is temperature dependent, studying the effects of temperature has both experimental and physiological relevance. An increase in temperature increases breathing frequency, but it may also have an effect on network dynamics. It is known that HFO peak frequency and temperature have a linear relationship of 5 Hz/$^\circ$C in a decerebrate cat preparation

(Richardson & Mitchell, 1982). Rats appear to maintain ~4Hz/$^{\circ}$C linear relationship between HFO and temperature (John & Leiter, 2003; Marchenko & Rogers, 2007), but the effects of temperature on MFO activity is not known.

In addition to endogenous changes, perturbations that change the intrinsic dynamics by changing the properties of the components of the respiratory rhythm generation center, there exist exogenous perturbations such as spontaneously occurring reflexes like micturition. The micturition reflex does share some muscle (external oblique) and neural components (periaqueductal grey) of the respiratory network, and yet previous studies have suggested that urinary bladder afferents can affect both respiration rate and amplitude (Gdovin, Knuth, & Bartlett, 1994; Schondorf & Polosa, 1980). Studies that have characterized respiratory neural output during spontaneous bladder contractions (SBCs) primarily have been conducted in decerebrate cats, although one study in decerebrate rats was conducted (M. Stella, Knuth, & Bartlett, 2000); thus, the relationship between SBCs and respiration is not well-characterized in the rat model.

The micturition reflex consists of two main phases: storage (continence) and evacuation (voiding, micturition). Sympathetic stimulation maintains internal urethral sphincter tone, allowing for urine storage. Sympathetic stimulation peaks during the guarding reflex, which occurs directly prior to active voiding. While filling, bladder stretch receptors activate afferents that project into the spinal cord and activate segmental reflexes to inhibit bladder contraction and stimulate EUS contraction. During active voiding the internal urethral sphincter relaxes due to parasympathetic stimulation to the detrusor muscle, which manifests as a series of bursts. The bladder also projects sensory information to the periaqueductal grey (PAG), which integrates sensory information from higher brain centers with bladder information. Projections from the

PAG activate the pontine micturition center, and this area initiates the switch from continence to active sustained contraction.

Specific Aims

Maintaining homeostasis is a necessity and non-trivial process for a properly functioning mammalian system. The respiratory neural control system, located in the brainstem, is key to maintaining homeostasis for important variables such as arterial blood gases and pH. To maintain these variables relatively constant in response to the myriad of exogenous and endogenous perturbations that can affect them, the respiratory control system produces and orchestrates various respiratory-related behaviors.

In addition, in order to compensate for perturbations on a breath-to-breath basis, the respiratory control system must be capable of making rapid adjustments, and it is therefore a relatively dynamical system/network. This control system exhibits both long-time-scale features that are associated with respiratory cycle timing (i.e., breathing frequency, f_b) and short-time-scale features (i.e., fast oscillatory rhythms) that are associated with intrinsic respiratory-related network interactions, which include inspiratory-related muscles, nerves and neurons. Thus, together these long- and short-time-scale features can be used to more comprehensively form a picture about the dynamics underlying various respiratory behaviors.

Perturbations to the respiratory network would be expected to produce a change in network configuration in order to elicit the necessary changes in respiratory output. While a variety of perturbations seemingly have a similar effect on respiratory modulation (e.g., increase or decrease respiratory frequency), it is expected that the source of the modulation differs, and the network configuration should change (e.g., recruiting, silencing, up-regulating or down-regulating specific neural populations within the respiratory network) due to the mechanics of the specific perturbation. Therefore, our overarching hypothesis is that perturbations cause a change in the underlying dynamics of the respiratory network by differentially affecting network reconfiguration.

To investigate this hypothesis, we present the following specific aims:

Specific Aim 1: Determine the effects of endogenous perturbations on the dynamics of the rodent respiratory neural network.

- **Sub-aim 1.** Using a reduced rodent preparation, we will examine the effects of altaring extracellular potassium concentration, which directly affects neuronal excitability, on temporal, spectral and information domain characteristics. We will also evaluate the phase relationship between multiple inspiratory neural outputs.
- **Sub-aim 2**. Using a reduced rodent preparation, we will investigate the effects of gradated temperature, which affects ionic kinetics to change excitability, on temporal, spectral and information domain characteristics of the respiratory neural network.

Specific Aim 2: Determine the effects of exogenous perturbations on the dynamics of the rodent respiratory neural network.

- Using an *in vivo* adult rodent preparation, we will examine the relationship between micturition and breathing; we will investigate the effects of micturition on breathing as well as the effect of increased respiratory drive on micturition

References

Chen, X., Solomon, I., & Chon, K. (2004). *Comparison of the use of approximate entropy and sample entropy: applications to neural respiratory signal.* Paper presented at the Conference proceedings:... Annual International Conference of the IEEE Engineering in Medicine and Biology Society. IEEE Engineering in Medicine and Biology Society. Conference.

Cohen, M. I., Piercey, M. F., Gootman, P. M., & Wolotsky, P. (1974). Synaptic connections between medullary inspiratory neurons and phrenic motoneurons as revealed by cross-correlation. *Brain research, 81*(2), 319.

Cohen, M. I., See, W. R., Christakos, C. N., & Sica, A. L. (1987). High-frequency and medium-frequency components of different inspiratory nerve discharges and their modification by various inputs. *Brain research, 417*(1), 148-152.

Funk, G. D., & Parkis, M. A. (2002). High frequency oscillations in respiratory networks: functionally significant or phenomenological? *Respiratory physiology & neurobiology, 131*(1), 101-120.

Gdovin, M., Knuth, S., & Bartlett, D. (1994). Respiratory motor nerve activities during spontaneous bladder contractions. *Journal of Applied Physiology, 77*(3), 1349-1354.

Hansen, A. J. (2008a). The extracellular potassium concentration in brain cortex following ischemia in hypo-and hyperglycemic rats. *Acta Physiologica Scandinavica, 102*(3), 324-329.

Hansen, A. J. (2008b). Extracellular potassium concentration in juvenile and adult rat brain cortex during anoxia. *Acta Physiologica Scandinavica, 99*(4), 412-420.

Holstege, G. (2013). The periaqueductal gray controls brainstem emotional motor systems including respiration. *Progress in brain research, 209*, 379-405.

John, W. M. S., & Leiter, J. (2003). High-frequency oscillations of phrenic activity in eupnea and gasping of in situ rat: influence of temperature. *American Journal of Physiology-Regulatory, Integrative and Comparative Physiology, 285*(2), R404-R412.

Lumsden, T. (1923). Observations on the respiratory centres in the cat. *The Journal of physiology, 57*(3-4), 153-160.

Marchenko, V., & Rogers, R. F. (2007). Temperature and state dependence of dynamic phrenic oscillations in the decerebrate juvenile rat. *American Journal of Physiology-Regulatory, Integrative and Comparative Physiology, 293*(6), R2323-R2335.

O'Neal, M. H., Spiegel, E. T., Chon, K. H., & Solomon, I. C. (2005). Time-frequency representation of inspiratory motor output in anesthetized C57BL/6 mice in vivo. *Journal of neurophysiology, 93*(3), 1762-1775.

Okada, Y., Kuwana, S., Kawai, A., Mückenhoff, K., & Scheid, P. (2005). Significance of extracellular potassium in central respiratory control studied in the isolated brainstem–spinal cord preparation of the neonatal rat. *Respiratory physiology & neurobiology, 146*(1), 21-32.

Pincus, S. M., & Huang, W. M. (1992). Approximate entropy: statistical properties and applications. *Communications in Statistics-Theory and Methods, 21*(11), 3061-3077.

Rekling, J. C., & Feldman, J. L. (1998). PreBötzinger complex and pacemaker neurons: hypothesized site and kernel for respiratory rhythm generation. *Annual review of physiology, 60*(1), 385-405.

Richardson, C. A., & Mitchell, R. A. (1982). Power spectral analysis of inspiratory nerve activity in the decerebrate cat. *Brain research, 233*(2), 317-336.

Richter, D. (1982). Generation and maintenance of the respiratory rhythm. *Journal of Experimental Biology, 100*(1), 93-107.
Richter, D., Ballantyne, D., & Remmers, J. (1986). How is the respiratory rhythm generated? A model. *Physiology, 1*(3), 109-112.
Schondorf, R., & Polosa, C. (1980). Effects of urinary bladder afferents on respiration. *Journal of Applied Physiology, 48*(5), 826-832.
Smith, J. C., Abdala, A., Koizumi, H., Rybak, I. A., & Paton, J. F. R. (2007). Spatial and functional architecture of the mammalian brain stem respiratory network: a hierarchy of three oscillatory mechanisms. *Journal of neurophysiology, 98*(6), 3370-3387.
Smith, J. C., Ellenberger, H. H., Ballanyi, K., Richter, D. W., & Feldman, J. L. (1991). Pre-Bötzinger complex: a brainstem region that may generate respiratory rhythm in mammals. *Science (New York, NY), 254*(5032), 726.
St-John, W. M. (1998). Neurogenesis of patterns of automatic ventilatory activity. *Progress in neurobiology, 56*(1), 97-117.
St John, W. M. (1985). Maintenance of respiratory modulation by pneumotaxic mechanisms in deep anesthesia. *Experimental neurology, 87*(2), 382-386.
Stella, G. (1938). On the mechanism of production, and the physiological significance of "apneusis". *The Journal of physiology, 93*(1), 10-23.
Stella, M., Knuth, S., & Bartlett, D. (2000). Respiratory response to spontaneous contractions of the urinary bladder in awake and decerebrate rats. *Respiration Physiology, 120*(2), 105-114. aa

Chapter 2: Effects of Temperature and Potassium on the Respiratory Neural Network

Introduction

The intrinsic properties of breathing rhythm generation often is studied in reduced animal preparations. These preparations are advantageous because they allow for increased control of many parameters including temperature, extracellular environment, vascular pressure, afferent and efferent contribution, etc. These preparations also allow specific networks to be selected as well. For instance, brain slice preparations allow specific areas of the brain to be accessed and tested while controlling inputs to the tissue or other variables such as temperature, extracellular ion concentrations, etc. However, because the preparation is reduced and many of the systems required to maintain viable tissue are removed, a variety of methods are used to alter the excitability of the tissue and prolong the viability of the experimental model. Two common methods of altering excitability are to lower tissue temperature and elevate $[K^+]_o$.

Most reduced preparations are conducted at temperatures much lower than normal physiological temperatures (~37˚C) to reduce tissue degradation by decreasing metabolic excitability and at potassium levels higher than normal physiological levels (~3.0 mM $[K^+]_o$ (Somjen 2002)) to compensate for the reduced excitability. For example*, in vitro* brainstem-spinal cord preparations and slice preparations are conducted in temperatures as low as 27˚C and are perfused with a solution where the $[K^+]_o$ typically is 9.0 mM, although it may be higher.

Elevating temperature and $[K^+]_o$ are known to increase excitability of the respiratory network. Increasing either parameter alters metrics of fictive breathing in ways consistent with increased drive to breathe (e.g., increased breathing frequency, decreased T_I and decreased time-to-peak activity) (Y. Okada, S. Kuwana, A. Kawai, K. Mückenhoff, & P. Scheid, 2005).

However, while it may appear that increasing temperature and $[K^+]_o$ have similar effects, the mechanism by which they modulate the respiratory network is not well-understood.

Increasing the temperature of the *in situ* perfusate increases fictive breathing frequency (W. M. St-John & Leiter, 2003) and increases neuronal excitability, evidenced by a linear shift HFO frequency by about 5 Hz/$^{\circ}$C in a decerebrate cat preparation (Richardson & Mitchell, 1982). Rats appear to maintain ~4Hz/$^{\circ}$C linear relationship between HFO and temperature (W. M. S. John & Leiter, 2003; Marchenko & Rogers, 2007), but the relationship between MFO and temperature remains unknown. Whether or not the network is reconfigured remains unexplored.

In reduced preparations, a high $[K^+]_o$ is used to increase the basal level of network excitability, although K^+ is known to have an important role in the generation of respiratory behavior. For instance, persistent K^+ ion channels have been shown to be critical to the respiratory pacemaker responsible for gasping (W. M. S.-. John, Rybak, & Paton, 2002) but is suppressed during eupnea (Butera Jr, Rinzel, & Smith, 1999; Rybak, Paton, Rogers, & St-John, 2002), illustrating an important role for K^+ in respiratory behavior. In the *in situ* preparation, while not statistically significant, trends of increased drive (e.g., decreased T_I and increased f_b) were observed as $[K^+]_o$ increased, (Y. Okada, S.-i. Kuwana, A. Kawai, K. Mückenhoff, & P. Scheid, 2005; W. St-John, Rudkin, Harris, Leiter, & Paton, 2005), although a significant change in expiratory duration, duty cycle or time-to-peak was not observed (W. St-John et al., 2005). It is not clear how or if changes in $[K^+]_o$ affect spectral and complexity-domain characteristics.

In addition to being experimentally relevant to understand the effects of these parameters on breathing with the purpose of understanding and interpreting literature, they also are physiologically relevant parameters. For example, fevers and hypothermia are naturally occurring situations where core body temperature is altered, and there exist a variety of disorders

that exhibit electrolyte imbalances, and alter $[K^+]_o$ away from physiological range, (e.g., kidney disease, diabetes, heart failure), and anoxic and ischemic conditions have been shown to alter $[K^+]_o$ on the surface of the brain cortex (Hansen, 2008a, 2008b).

In order to understand the effects of changes in temperature and $[K^+]_o$ on the respiratory network, we selected the *in situ* arterially-perfused preparation. This preparation is advantageous not only due to the presence of an intact brainstem but also because it allows for controlled and precise alterations to both temperature and $[K^+]_o$ of the tissue, and, therefore, is suitable to test the hypothesis that, because these two perturbations modulate general excitability of the neurons, the underlying network and their connections will remain similar.

Methods

Methods for the changes in temperature studies

Experiments were conducted in 38 adolescent (~4-5 weeks old) Sprague-Dawley rats in a modified arterially-perfused rat preparation (Paton). Adolescent (~4-5 weeks old; n=38) Sprague-Dawley rats were deeply anesthetized using isoflurane (2-5%) via inhalation until respiration ceased. After testing for the absence of a withdrawal reflex in response to a noxious paw pinch, the rat rapidly was sub-diaphragmatically transected and submerged in an ice-cold bath of artificial cerebral spinal fluid (aCSF (in mM): 125 NaCl, 24 $NaHCO_3$, 5.0 KCl, 2.5 $CaCl_2$, 1.25 $MgSO_4$, 1.25 KH_2PO_4, and 10 glucose) bubbled with % O_2-5% CO_2. The skull was removed, the animal was decerebrated at the pre-collicular level, the skin and lungs were removed, and the thoracic aorta was separated from the vertebral column. It should be noted that a decerebration at this level removes the brain centers involved in the sensation and perception of pain, and therefore no supplemental anesthesia is necessary. The preparation was moved to a recording chamber where the descending thoracic aorta was cannulated with a double-lumen

catheter; French 3.5). One lumen of the catheter was used to perfuse the preparation with a modified aCSF (2.5% Ficoll, an oncotic agent, is added; Sigma Chemical, St. Louis, MO) by a peristaltic pump (PeriStar, World Precision Instrument, Sarasota, FL). The perfusate was gassed continuously with 95%O_2-5%CO_2, warmed in a water bath such that the perfusate in the cranial vault will be ~31˚C, filtered through a nylon mesh (pore size: 40 μm; Millipore, Bedford, MA) and passed through a bubble trap to remove gas bubbles and mitigate pulsations due to the pump. The other lumen of the catheter was connected to a pressure transducer to continuously measure perfusion pressure. Pressure gradually was increased until phrenic nerve activity becomes eupneic-like (*i.e.,* "ramp-like"), and pressure was maintained throughout the remainder of the experiment. Prior to recording, vecuronium bromide (2 mg) was added to the perfusate to eliminate motor movements associated with respiratory efforts.

Recording protocol

Baseline phrenic and XII data was recorded at temperatures typical for *in situ* preparations (~31˚C) for at least 10 minutes and until the neural output was stable. Perfusate temperature was cooled to the low temperature (LT) condition (~28˚C), recovered back to basal temperatures increased to the high temperature (HT) condition (~37˚C) then recovered again (Series 3: n_{Phr}=15, n_{XII}=6),. Two other series of experiments were conducted: baseline data was collected and then the perfusate either was decreased (Series 1: n_{Phr}=14, n_{XII}=10) or increased (Series 2: n_{Phr}=9, n_{XII}=8), then allowed to recover. Temperature changes were achieved by placing a heating coil in different temperature water baths. The LT and HT conditions were recorded until the temperature of the cranial vault remained stable for at least 3 minutes (~10 minutes). Between conditions the preparation was allowed to recover for at least 20 minutes.

Methods for changes in [K+]o series

Experiments were conducted in 49 adolescent (~4-5 weeks old) Sprague-Dawley rats in a modified aterially-perfused rat preparation (Paton). Adolescent (~4-5 weeks old) Sprague-Dawley rats were deeply anesthetized using isoflurane (2-5%) via inhalation until respiration ceased. After testing for the absence of a withdrawal reflex in response to a noxious paw pinch, the rat rapidly was sub-diaphragmatically transected and submerged in an ice-cold bath of artificial cerebral spinal fluid (aCSF (in mM): 125 NaCl, 24 $NaHCO_3$, 2.5 $CaCl_2$, 1.25 $MgSO_4$, 1.25 KH_2PO_4, and 10 glucose) containing the lowest concentration of K^+ used in the experimental protocol and bubbled with % O_2-5% CO_2. Four solutions of aCSF comprising different levels of total [K^+] were used: 3.0, 4.25, 6.25, and 9.0 mM. In experiments using either 3.0 or 4.25 mM [K^+], choline chloride was used to obtain a solution equimolar to the 6.25 mM K_+ aCSF, and in experiments using aCSF with 9.0 mM $[K^+]_o$, additional KCl was added. The osmolality of the solutions were measured (Advanced Instruments Osmometer Model 3320, Norwood, MA) to ensure similar osmolality. The preparation was prepared in the aCSF containing the lowest concentration of K^+ used in the experimental protocol, the exception being that experiments that used 9.0 mM K^+ were prepared in 6.25 mM K^+ aCSF. The skull was removed, the animal was decerebrated at the pre-collicular level, the skin and lungs were removed, and the thoracic aorta was separated from the vertebral column. It should be noted that a decerebration at this level removes the brain centers involved in the sensation and perception of pain, and therefore no supplemental anesthesia is necessary. The preparation was moved to a recording chamber where the descending thoracic aorta was cannulated with a double-lumen catheter; French 3.5). One lumen of the catheter was used to perfuse the preparation with a modified aCSF (2.5% Ficoll, an oncotic agent, was added; Sigma Chemical, St. Louis, MO) by a peristaltic pump (PeriStar, World Precision Instrument, Sarasota, FL). The perfusate was gassed

continuously with 95%O_2-5%CO_2, warmed in a water bath such that the perfusate in the cranial vault will be ~31°C, filtered through a nylon mesh (pore size: 40 μm; Millipore, Bedford, MA) and passed through a bubble trap to remove gas bubbles and mitigate pulsations due to the pump. The other lumen of the catheter was connected to a pressure transducer to continuously measure perfusion pressure. Pressure gradually was increased until phrenic nerve activity becomes eupneic-like (*i.e.,* "ramp-like"), and pressure was maintained throughout the remainder of the experiment. Prior to recording, vecuronium bromide (2 mg) was added to the perfusate to eliminate motor movements associated with respiratory efforts

Two series of experiments were conducted. In the first series, four groups corresponding to each level of $[K^+]_o$ were studied separately; the groups were: 3.0, 4.25, 6.25 and 9.0 mM $[K^+]_o$(3.0 mM n=7; 4.25 mM n=7; 6.25 mM n=7; 9.0 mM n=6). In each experiment, baseline PHR and XII nerve discharge were recorded, and the last 10 basal inspiratory bursts were used for data analysis. In the second series, the effects of increasing the $[K^+]_o$ level were examined using a paired experimental design with the following groups:

Group	Baseline $[K^+]_o$ (mM)	2nd $[K^+]_o$ (mM)	3rd $[K^+]_o$ (mM)
1	3.0	6.25	3.0
2	6.25	9.0	6.25
3	3.0	6.25	9.0

At least 10 minutes of baseline data was collected. The perfusate was switched to a flask with the 2nd aCSF until the preparation stabilized (about 15-20 minutes), and then the perfusate either

was switched back and allowed to recover, or was switched to a higher K^+ aCSF. To achieve gasping behavior, a second series of experiments (3.0 mM n=7; 6.25 mM n=7; 9.0 mM n=7) were conducted where only phrenic nerves were isolated, and the experiment was terminated by an anoxic challenge achieved by rerouting the perfusate away from the animal.

Data acquisition

One or both phrenic nerves were dissected from the surrounding connective tissue and sectioned at the insertion point on the diaphragm. Phrenic nerve activity was recorded using bipolar hook. In a subset of these experiments XII nerve discharge simultaneously were isolated and recorded. Phrenic and XII nerve discharged was be amplified (x10k) and filtered (10 Hz to 1 kHz) and a moving average obtained using a third-order Paynter filter with a 50 ms time constant. Both raw and averaged phrenic nerve activity were recorded digitally (sampling rate of 2 kHz; Chart 4.0, PowerLab, ADInstruments, Colorado Springs, CO) and digital tape (DAT, Cygnus, Delaware Water Gap, PA). Early data (Series 1: n=3, Series 3: n=7) collected in the temperature-series of experiments included a 60 Hz notch filter. Due to concerns that the filter was obscuring changes in MFO frequency, the filter was removed for subsequent experiments. These data were included in temporal analyses but not included in spectral analyses. A 60 Hz notch filter, however, was used for the potassium-series of experiments.

Data Analysis and Statistics

T_{Phr}, T_E and T_{XII} were calculated from phrenic nerve activity: T_{Phr} was defined as the duration of phrenic nerve activity; T_E was defined as the T_{XII} was the duration of any XII activity. Pre-inspiratory (PreI) activity is the difference between the onset of XII and phrenic nerve activities. Approximate entropy (ApEn) values were calculated as previously published (Pincus, 1991). Data are the average of the last 10 inspiratory bursts of each condition.

Complexity-domain analysis was calculated using the approximate entropy (Pincus, 1991) algorithm where m=3 and r=0.3 (Lu, Chen, Kanters, Solomon, & Chon, 2008).

Frequency domain was performed with time-invariant and time-varying methods. These data were segmented into lengths of 256 data points and zero-padded if necessary yielding 1.95 Hz resolution. The data then was digitally band-pass filtered between 20 (to minimize frequencies associated with ECG) and 250 Hz using a Hanning window. Specifics for the power spectral density (time-invariant) and smoothed-pseudo Wigner-Ville (time-varying) analyses were performed as previously published (O'Neal III, Spiegel, Chon, Solomon, & Solomon, 2004).

Statistics for the Series 1 and 2 temperature experiments were performed using paired t-test (α=0.05). Statistics for the Temperature Series 3 experiments were performed using a one-way repeated measures ANOVA (α=0.05) with a Holm-Sidak post-hoc test. Statistics between different levels of $[K^+]_o$ were performed using a one-way ANOVA (α=0.05). Statistics for experiments where more than 1 level of $[K^+]_o$ was tested were performed using a one-way repeated measures ANOVA (α=0.05). For both temperature and K^+ experiments, a paired-t-test was used to compare Phr and XII activity in the tested condition. All values are reported as mean±SE. Coefficient of variation (CV) was calculated as the ratio of standard deviation over the mean. All values are reported as mean±SE.

Results for temperature experiments

The temperatures for each series of temperature experiments were conducted at similar temperatures for their conditions (Table 1). Raw traces from a single experiment (Figure 1) show the effect of temperature on breathing. All experiments maintained a regular, augmenting respiratory discharge pattern. It was noted that an increase in temperature increased the

occurrence of non-respiratory-related XII neural discharge that recovered when temperature was lowered. Temperature did not have a significant effect on the amplitude of Phr nerve discharge, and in some cases it was observed that XII nerve amplitude decreased when in HT conditions. The raw traces also show that breathing frequency (f_b) was altered by temperature as expected; that is, breathing frequency increased as temperature increased and vice versa (LT≈12, BL≈16 and HT≈27 bpm) (summarized in Figure 2). There is considerable overlap between the f_b different temperature groups, and the change in f_b can be attributed to decreases in both T_I (LT≈0.92, BL≈0.68 and HT≈0.57 sec) and T_E (LT≈4.42, BL≈3.32 and HT≈2.03 sec). While the variability in the BL and LT groups are similar, but the variability for the HT group is larger, and the variability is due to the increase in variability in both T_I (CV_{LT}≈23.5%, CV_{BL}≈23.0% and CV_{HT}≈43.8%) and T_E (CV_{LT}≈41.6%, CV_{BL}≈36.0% and CV_{HT}≈61.1%). Unlike Phr activity, variability in XII activity (T_{XII}) during the high temperature decreased significantly. Duty cycle for both Phr and XII nerve output remained similar over the span of temperatures tested **(**Figure 3**)**, which indicates that neither T_I nor T_E had a dominant role in changing f_b. PreI XII neural activity was observed to be largely variable not only in duration but also in quality of the signal during lower temperatures in particular; breaths with long PreI neural activity often had spurious discharges of neural activity instead of more synchronized activity. PreI duration between LT and NT were similar to each other, but both were significantly different from the HT group ($P<0.01$), resulting in XII duty cycles between LT and NT being statistically significant ($P<0.03$) from each other. PreI duration change was non-linear and may be the driving difference for the non-linear change in XII duty cycle.

Complexity

Summary ApEn values (Figure 4) for both phrenic and XII activity with respect to temperature for the non-control experiments show that temperature has an effect on network complexity. ApEn values for Phr nerve activity in for low and baseline temperatures were significantly different from the high temperature group, but none of the ApEn values for XII nerve activity were significantly different. However, like the temporal data, there is considerable overlap between all the groups. When comparing ApEn values between nerves, ApEn values were significantly different for the LT (Phr=0.78±0.01; XII=0.72±0.02) and BL (Phr=0.77±0.01; XII=0.72±0.01) groups and not significant for the HT group (Phr=0.72±0.02; XII=0.720±0.02), and the difference between in ApEn values between the two nerves decreases as temperature increases. In general, ApEn values for XII neural output was more variable for a given temperature compared to Phr neural output, particularly in the LT and BL conditions.

Spectral Analysis

In addition to changes in the temporal and information domain, temperature changed phrenic nerve output in the spectral domain (Figure 5). In the example power spectral density (PSD) graph from a single experiment, two dominant peaks consistently were observed, the lower being in the medium frequency oscillation (MFO) range (classically defined to be 40-50 Hz) and the higher being in the high frequency oscillation (HFO) range (classically defined as 90-110). In some cases, particularly in the HT group, more than one dominant peak in the HFO range was observed, and in these cases the largest peak was used. Because temperature has an effect on the frequency of the dominant peak, these ranges were expanded (MFO: 20-70Hz; HFO:70-150Hz) to accommodate the change. The ratio of the powers of the MFO and HFO dominant peaks a significant difference between the LT (1.30±0.15) and the other two groups (BL=0.53±0.07; HT=0.53±0.20). This suggests that there is possibly is a shift from motoneuron-

dominated rhythm generation to a more medullary-dominated rhythm generation as temperature increases. With respect to the frequency of these dominant peaks, spectral analysis revealed that a ~4.2 Hz/$^{\circ}$C linear relationship exists between the HFO dominant peak and temperature for the range of temperatures tested. The effect of temperature on the frequency of the MFO dominant peaks is less clear. While the location (frequency) of the peak does not change significantly as a group, the variability increases greatly as temperature increases. The MFO peak also does not seem to increase linearly; a linear regression produves an R^2-value of 0.12.

To provide insight into the non-stationary characteristics of Phr nerve discharge, we used time-varying analysis to produce time-frequency (TF) spectrum. A TF spectrum was generated for each breath, normalized to account for varying T_{Phr} In the TF spectrum heat maps, dark blue is 0 activity and dark red is maximal activity. The top panel of Figure 6 shows the TF spectrum on their own relative scale for the 3 temperature categories from a single experiment. The TF spectrum echo the results seen in the PSD analysis: there is a trade-off in power from MFO activity to HFO, and it also shows the increase in the frequency of HFO peak activity as temperature increases. These TF spectrum reveal, however, that the HFO peak frequency shifts to an earlier time within the burst as temperature increases, and that significant activity in the high frequency range (60% and above; i.e., light green to red activity) becomes more concentrated in both the time and frequency domains, potentially indicating a more synchronized network. The bottom panel shows the TF spectrum normalized to the highest power of the entire experiment. In this particular experiment HFO peak power was less than the MFO peak power. Figure 8 shows the time course of the same experiment as Figure 7 and illustrates how dynamic the system is. TF spectrum of the last 10 breaths for each minute normalized to the highest power of the entire experiment was combined and presented to show the TF spectrum over the course of

an entire experiment. Even though this experiment was conducted with a 60 Hz notch filter, the dynamic nature of the preparation. HFO frequency is altered with temperature, and the ramping of the frequency reflects the gradual change in temperature of the perfusate. This contour plot more clearly shows the change in the spread of HFO activity; it is more dispersed in the LT condition and more concentrated in the HT condition. The increase in MFO activity during the LT condition and decrease in the MFO activity during the HT condition also is evident. It was observed that, when the temperature increased, there was an initial overshoot in the response in the HFO range, whether it be an overshoot in power or frequency, that recovers as the temperature change stabilizes. For example, the initial minute of the recovery condition exhibits a response to the change in temperature with a large increase in HFO power that ultimately decreases as at the end of the recovery condition. The activity in the range of the MFO did not exhibit an overshoot but did take time to stabilize.

Results: Effect of $[K^+]_o$ on Phrenic and XII output

Example traces of phrenic and XII activity recorded simultaneously under different concentrations of $[K^+]_o$ (Figure 8) shows that changing the levels of K_+ had an effect on fb (3.0 mM: ~14, 4.25 mM: ~17, 6.25 mM: ~17, 9.0 mM: ~ 22 bpm), although the change was slight aside from the 9.0 mM group, which had a significantly higher f_b than the other groups. Altering the $[K^+]_o$ did not alter the appearance of phrenic nerve output significantly: amplitude did not change significantly in experiments with more than 1 level of [K+], and the bursts still exhibited characteristics typical of respiratory neural discharge in an in situ preparation which include an abrupt onset with regular, augmenting respiratory discharge pattern. The bottom panel shows an example burst from each level of K+. XII burst shapes were rather variable even within groups, but in general had a more gradual onset than a phrenic burst and varied between an augmenting

and more square-wave type shape. Summary of burst durations (Table 2) of both Phr and XII, where the latter has been split into the duration of just the preI period and the entire burst activity. Pre-I duration (3.0: 796±42; 4.25: 684±29; 6.25: 718±41; 9.0: 595±34 mS) was not significantly different between any of the groups (3.0: 229±42; 4.25: 200±22; 6.25: 235±50; 9.0: 188±32 mS), but the 3.0 and 6.25 mM groups were significantly different from the 9.0 mM group for both Phr and XII nerve output, indicating that the difference in XII durations is driven by inspiratory duration and not PreI. TE (3.0: 2.95±0.26; 4.25: 3.55±0.24; 6.25: 2.50±0.27; 9.0: 2.27±0.11 sec) was significantly different when comparing the 4.25 mM group to the 6.25 and 9.0 mM groups, which suggests that the significant change in f_b is driven mostly by changes in T_I.

To gain insight into whether these changes in temporal characteristics were a result of network configuration, time-invariant, time-varying spectral analyses and approximate entropy calculations were performed. Unlike the temperature studies, example PSD and TF plots taken from 2 different experiments (one that involved a flask switch from 3 mM to 6.25 mM $[K^+]_o$ and another that involved a flask switch from 6.25 to 9.0 mM $[K^+]_o$) showed that there was no significant change in either spectral activity across K^+ levels (Figure 9). The top panels, which are PSD overlays from Phr nerve data from the two conditions, show that not much changed in the time-invariant spectral analyses; power, frequency nor width of the dominant medium frequency oscillations (MFO; classically defined to be in the 40-50 Hz range) or high frequency oscillations (HFO; classically defined to be in the 70-120 Hz range) had significant differences. Spectral analysis was not performed on XII nerve output due to lack of consistent peaks akin to MFO and HFO dominant peaks. The bottom panel, which shows the TF spectrum, illustrate that the timing of when these dominant frequencies occur during a burst also are not significantly

different; the activity of the dominant peak (red) occurs at similar times, and they also contain similar background (green to light blue) activity in shape and concentration. These analysis could indicate that the network is conserved when $[K^+]_o$ is changed.

ApEn values (Figure 10), however, indicate that there may be some network configuration. ApEn values of the Phr nerve output to just the inspiratory portion of XII data (XII_I) for the unpaired series of data. When comparing ApEn values of Phr nerve activity (3.0: 0.82±0.01; 4.25: 0.78±0.01; 6.25: 0.79±0.01; 9.0: 0.75±0.01 mS), there were significant differences ($P<0.05$) between the 3.0 and 4.25 mM, 3.0 and 9.0 mM, and 6.25 and 9.0 mM groups. When comparing the XII_I, no statistical difference was detected between the groups, but the 4.25 and 9.0 mM groups showed statistical difference between Phr and XII_I. In all groups ApEn values for Phr nerve output was lower than that of XII_I, which indicates that the signal from the Phr is more orderly than the inspiratory portion of XII nerve output. Figure 11 separates and compares the XII burst into 3 components: PreI portion (XII_P), inspiratory portion (XII_I), and the entire XII burst (XII_{P+I}). The ApEn values for the PreI portion was significantly lower ($P<0.001$) regardless of $[K^+]_o$ than the ApEn values calculated for the other nerve phases, suggesting that the PreI portion of a XII burst may have a different network than the inspiratory part. The significantly lower ApEn values account for XII_{P+I} values being slightly lower than XII_P values.

Discussion

Our hypothesis, that changing the intrinsic properties of neurons such that they are more or less excited will modify the output but not change the organization of the underlying respiratory network, was partially correct; while $[K^+]_o$ did not appear to change the organization of the underlying respiratory network, changes in temperature did. We explored this hypothesis

under two different modes of excitability (temperature and $[K^+]_o$) in 2 ways: we looked at the effects of these perturbations on a given neural output, and we looked at the relationship between the Phr and XII nerves. Within a given nerve, we saw that, while both perturbations resulted in an overall excitatory effect, that is, as temperature or $[K^+]_o$ increased, both the orderliness of the inspiratory breaths and breathing frequency increased, although it should be noted that a 3-fold $[K^+]_o$ increase from physiological range was necessary to see a change in breathing frequency.. However, these two perturbations differed with respect to their effect on spectral characteristics; whereas a change in temperature elicited a shift in HFO peak frequency and MFO and HFO power contributions, a change in $[K^+]_o$ did not elicit a significant change in spectral dynamics. Between nerves we saw that the temporal relationship between the onsets of Phr and XII nerve activity were similar for temperatures well below physiological temperature but decreased at a different rate when closer to the physiological range and remained largely unaffected by changes in $[K^+]_o$. With respect to the orderliness of inspiratory breaths, Phr and XII signal were statistically different from each other under all conditions, but they did not did not respond similarly to changes in temperature or $[K^+]_o$.

Our data is consistent with previous temperature experiments that have shown that breathing frequency increases non-linearly in both cats and guinea pigs, with the rate of rise increasing around 35˚C (Barcroft & Izquierdo, 1931). Because the *in situ* preparation does not involve feedback or use of the upper airways, this non-linear change is not fully explained by the inhomogeneity of the upper airways or a chance in resistance or elasticity of the airways (Rubini & Bosco, 2013), but instead is central in origin. Having a change in slope at 35˚C is not completely unexpected since this temperature generally is accepted to be the threshold for hypothermia, where the temperature is not high enough to maintain normal metabolism.

Furthermore, the ideal gas law indicates that kinetics of ions change linearly with temperature, so this non-linear relationship may suggest that 35˚C is a critical temperature for a channel to remain thermally stable. The change in slope of breathing frequency across the temperature range observed indicates that temperature does not simply change the basal level of excitability of the respiratory network.

Further supporting the idea that temperature changes or reconfigures the respiratory network is the change in MFO power relative to HFO power. Our data agree with previous experiments in cats and rats (Marchenko & Rogers, 2007; Richardson & Mitchell, 1982; W. M. St-John & Leiter, 2003) that there is a temperature-dependent shift in the frequency of the dominant HFO peak, and the slope, in this case ~4Hz/˚C, may be species dependent. A shift in frequency, especially one driven by temperature, does not necessarily indicate that there has been network reorganization, for temperature merely could be exciting the same network such that it fires at a faster rate due to a temperature-dependent change in kinetic energy. However, the change in dominant spectral activity between MFO and HFO ranges strongly suggests that some network reorganization exists, since HFO and MFO peaks are believed to originate from motoneuron and medullary contributions (Chritaakos, Cohen, See, & Barnhardt, 1988; Cohen, See, Christakos, & Sica, 1987). It is possible that the decrease in complexity as temperature increases is a result of the HFO dominance in the signal, since HFO peaks are much more coherent than MFO peaks (Marchenko & Rogers, 2007). Further supporting the idea that there is network reorganization is the change in frequencies present, i.e., the spread of the frequencies active overall is larger at lower temperatures than it is at higher temperatures, and the spread in both time and frequency of the peak activity follow the same pattern. Due to the similarities in temporal characteristics between temperature groups, one possible interpretation of the spectral

data is that the medullary and motoneurons work together as potentially compensatory mechanisms to mitigate effects from perturbations to homeostasis.

Breathing frequency similarly is increased by increasing $[K^+]_o$ to modulate baseline membrane potential and increase breathing frequency (Johnson, Koshiya, & Smith, 2001). Studies have suggested that this method of increasing breathing frequency had very little effect on other characteristics of eupnea, including burst shape and general functionality (Del Negro, Kam, Hayes, & Feldman, 2009; W. St-John et al., 2005). Our results largely agree with these findings. Temporal analysis revealed that both phrenic and XII burst timing remained similar regardless of $[K^+]_o$. Additionally, $[K^+]_o$ had even less of an effect on the preI duration of XII nerve activity, although values at the 9.0 mM range do seem drop compared to the rest of the data. We saw a general trend toward increasing f_b, but the burst shapes largely remained similar, and spectral characteristics for phrenic nerve activity also remained similar regardless of $[K^+]_o$ in both the time-invariant and time-varying domains. These data suggest that using $[K^+]_o$ is a suitable method for increasing respiratory frequency without changing the underlying dynamics of the system significantly (i.e., K^+ changes the basal excitability of the neural network but may not reorganize it).

Because we know the respiratory network is a dynamic process, we used ApEn to try to capture some idea of the dynamic process. ApEn, which quantifies the predictability of a signal, can give insight into whether new information is being added to the signal. At the lower temperatures, ApEn values indicated that there was no significant change in information for the lower temperatures, but compared to the more physiological temperature, there was a significant change. The difference could be attributed to the metabolic changes due to hypothermia, and it further supports the idea that 35˚C is a critical temperature for the network. Our results with

respect to orderliness contradict the findings of Marchenko and Rogers (Marchenko & Rogers, 2007) who reported a dramatic increase in complexity with temperature when using spectral entropy (Rezek & Roberts, 1998) as their method of assessing complexity. In our studies we observed a decrease in complexity using ApEn analysis. It is difficult to assess the reliability of their measure due to a lack of details on some parameters necessary for the algorithm. While ApEn considers the predictability of the signal in the time domain, spectral entropy measures how sinusoidal a signal is and not how regular or predictable the signal is, which is how the authors incorrectly interpret their spectral entropy values. Therefore, an alternate interpretation of their increase in spectral complexity is that, due to a more synchronized network, additional peaks now are discernible.

Similarly, ApEn values suggest a trend that network complexity decreases in both neural outputs (Phr and XII) as $[K^+]_o$ levels increase. The difference in ApEn values is slight, however, further supporting the idea that K^+ changes basal network excitability instead of reorganizing it. While the change in ApEn decreases overall, the data show that the changes in information in the signals is greater (and statistically significant) in phrenic nerve output compared to XII nerve output, which may be due to the contribution of neurons activated during the PreI phase that contribute less of a change in network dynamics, supporting the idea Phr and XII (J. Peever, Shen, & Duffin, 2002) have different pre-motorneuron control since the spectral data indicate that the change in breathing frequency is not a result of the contributions of medullary or motoneuron components. The supposed discrepancy between the very similar spectral behavior and increase in orderliness could potentially be due to inactivation of Na^+ channels due to the elevated $[K^+]_o$.

The changes in the quality of the neural activity of the XII Pre-I during low temperatures could be a result of a limitation of the study, which is the assumption that perfusion level remains constant throughout the experiment. Due to temperature-dependent elasticity of the vasculature it is possible that the brainstem became less perfused due to vasoconstriction. The changes in physiological parameters affecting perfusion of the brainstem could also account for the inability for the animal to recover after a HT perturbation. It should be noted that we are invoking changes in temperature very quickly, which most likely is stimulating inflammatory responses, particularly when increasing the temperature, which also will affect the elasticity of the vasculature. While temporal analysis parameters for XII follow the same trend as Phr activity, we saw an opposite trend in variability between the 2 neurons - while the variability of Phr activity increased at higher temperatures, it decreased for XII - supporting the idea that XII and Phr are differentially controlled (J. H. Peever, Mateika, & Duffin, 2001). While we do see some changes in Pre-I activity qualitatively - the onset of XII activity in higher $[K^+]_o$ is more abrupt - our analysis did not extrapolate any real significant difference.

Conclusion

While temperature and K^+ both increased excitability of the respiratory network, that is, they both increased breathing frequency, our data suggest that they modulate the respiratory network differently. Even both perturbations are systemically induced, they do not merely increase basal excitability. It is necessary to balance the different perturbations to excitability, but it also is important to take note how these perturbations are functioning.

Our data suggest that specifics in the protocol for the *in situ* preparation are very important to consider and can have important implications on the parameters that may change with a perturbation (e.g., increasing vascular flow may change temperature of the perfusate).

Because the *in situ* preparation has had much of the excitatory matter removed, there is tuning that occurs before baseline recording which, in most cases, is not reported. While the *in situ* preparation allows for more control over a variety of parameters, it also introduces an experimenter's bias of what is a "normal" baseline. We suggest that more rigorous control and reporting of parameters may be necessary to have a consistent baseline. Our data indicate that the variability associated with all measurements related to phrenic nerve activity was larger in temperatures greater than 35˚C, therefore, we suggest that this temperature is the upper limit for studying a regular system or the lower limit for studying a physiologically relevant system. Our data also suggest that the *in situ* preparation withstands (i.e., recovers more completely and does not exhibit an overshoot when adjusting to the new condition) decreases in temperature better than increases in temperature. Lastly, our results suggest that there is a range of elevated $[K^+]_o$ that is suitable and experimentally advantageous. We would suggest that a total concentration of 9.0 mM $[K^+]$ is too high and may be altering the underlying network that generates respiration, particularly for studying phrenic nerve discharge.

References

Barcroft, J., & Izquierdo, J. (1931). The effect of temperature on the frequency of heart and respiration in the guinea-pig and cat. *The Journal of physiology, 71*(4), 364-372.

Butera Jr, R. J., Rinzel, J., & Smith, J. C. (1999). Models of respiratory rhythm generation in the pre-Bötzinger complex. I. Bursting pacemaker neurons. *Journal of neurophysiology, 82*(1), 382-397.

Chritaakos, C. N., Cohen, M. I., See, W. R., & Barnhardt, R. (1988). Fast rhythms in the discharges of medullary inspiratory neurons. *Brain research, 463*(2), 362-367.

Cohen, M. I., See, W. R., Christakos, C. N., & Sica, A. L. (1987). High-frequency and medium-frequency components of different inspiratory nerve discharges and their modification by various inputs. *Brain research, 417*(1), 148-152.

Del Negro, C. A., Kam, K., Hayes, J. A., & Feldman, J. L. (2009). Asymmetric control of inspiratory and expiratory phases by excitability in the respiratory network of neonatal mice in vitro. *The Journal of Physiology, 587*(6), 1217-1231.

Hansen, A. J. (2008a). The extracellular potassium concentration in brain cortex following ischemia in hypo-and hyperglycemic rats. *Acta Physiologica Scandinavica, 102*(3), 324-329.

Hansen, A. J. (2008b). Extracellular potassium concentration in juvenile and adult rat brain cortex during anoxia. *Acta Physiologica Scandinavica, 99*(4), 412-420.

John, W. M. S.-., Rybak, I. A., & Paton, J. F. (2002). Potential switch from eupnea to fictive gasping after blockade of glycine transmission and potassium channels. *American Journal of Physiology-Regulatory, Integrative and Comparative Physiology, 283*(3), R721-R731.

John, W. M. S., & Leiter, J. (2003). High-frequency oscillations of phrenic activity in eupnea and gasping of in situ rat: influence of temperature. *American Journal of Physiology-Regulatory, Integrative and Comparative Physiology, 285*(2), R404-R412.

Johnson, S. M., Koshiya, N., & Smith, J. C. (2001). Isolation of the kernel for respiratory rhythm generation in a novel preparation: the pre-Bötzinger complex "island". *Journal of neurophysiology, 85*(4), 1772-1776.

Lu, S., Chen, X., Kanters, J. K., Solomon, I. C., & Chon, K. H. (2008). Automatic Selection of the Threshold Value for Approximate Entropy. *Biomedical Engineering, IEEE Transactions on, 55*(8), 1966-1972.

Marchenko, V., & Rogers, R. F. (2007). Temperature and state dependence of dynamic phrenic oscillations in the decerebrate juvenile rat. *American Journal of Physiology-Regulatory, Integrative and Comparative Physiology, 293*(6), R2323-R2335.

O'Neal III, M. H., Spiegel, E. T., Chon, K. H., Solomon, I. C., & Solomon, I. C. (2004). Time-frequency representation of inspiratory motor output in anesthetized C57BL/6 mice in vivo.

Okada, Y., Kuwana, S.-i., Kawai, A., Mückenhoff, K., & Scheid, P. (2005). Significance of extracellular potassium in central respiratory control studied in the isolated brainstem–spinal cord preparation of the neonatal rat. *Respiratory physiology & neurobiology, 146*(1), 21-32.

Okada, Y., Kuwana, S., Kawai, A., Mückenhoff, K., & Scheid, P. (2005). Significance of extracellular potassium in central respiratory control studied in the isolated brainstem–

spinal cord preparation of the neonatal rat. *Respiratory physiology & neurobiology, 146*(1), 21-32.
Peever, J., Shen, L., & Duffin, J. (2002). Respiratory pre-motor control of hypoglossal motoneurons in the rat. *Neuroscience, 110*(4), 711-722.
Peever, J. H., Mateika, J. H., & Duffin, J. (2001). Respiratory control of hypoglossal motoneurones in the rat. *Pflügers Archiv, 442*(1), 78-86.
Pincus, S. M. (1991). Approximate entropy as a measure of system complexity. *Proceedings of the National Academy of Sciences, 88*(6), 2297-2301.
Rezek, I., & Roberts, S. J. (1998). Stochastic complexity measures for physiological signal analysis. *IEEE Transactions on Biomedical Engineering, 45*(9), 1186-1191.
Richardson, C. A., & Mitchell, R. A. (1982). Power spectral analysis of inspiratory nerve activity in the decerebrate cat. *Brain research, 233*(2), 317-336.
Rubini, A., & Bosco, G. (2013). The effect of body temperature on the dynamic respiratory system compliance–breathing frequency relationship in the rat. *Journal of biological physics, 39*(3), 411-418.
Rybak, I. A., Paton, J. F., Rogers, R., & St-John, W. (2002). Generation of the respiratory rhythm: state-dependency and switching. *Neurocomputing, 44*, 605-614.
St-John, W., Rudkin, A., Harris, M., Leiter, J., & Paton, J. (2005). Maintenance of eupnea and gasping following alterations in potassium ion concentration of perfusates of in situ rat preparation. *Journal of neuroscience methods, 142*(1), 125-129.
St-John, W. M., & Leiter, J. (2003). High-frequency oscillations of phrenic activity in eupnea and gasping of in situ rat: influence of temperature. *American Journal of Physiology-Regulatory, Integrative and Comparative Physiology, 285*(2), R404-R412.

Figure 1 Example *in situ* raw and integrated phrenic and XII neural recordings in response to temperature.

Simultaneous recordings from both phrenic and XII nerve output from a single experiment. The temperatures reported correspond to the temperature of the perfusate in the cranial vault. While f_b was altered in the direction of temperature change and recovered in response to the perturbation, amplitude of either nerve was not affected by a change in temperature.

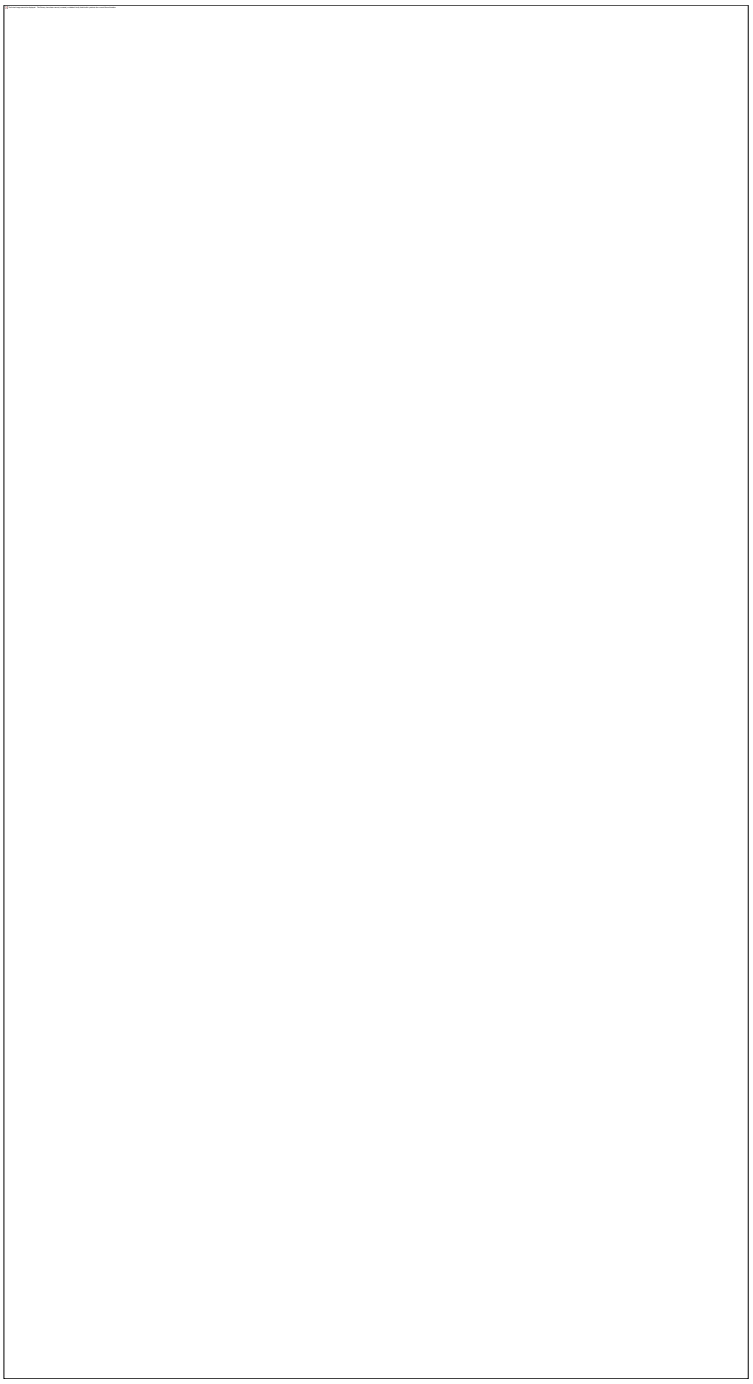

Figure 2 Summary data of temporal characteristics of phrenic and XII activity across temperatures.

Summary data from all experiments. f_b increases as temperature increases as a result of both T_{Phr} and T_E decreasing. T_{XII} also decreases, but at a faster rate than $T_{Phr,}$ which can be explained by the slight decrease in Pre-I as temperature increases. Open circles denote data from Series 1 and 2; filled circles denote data from Series 3.

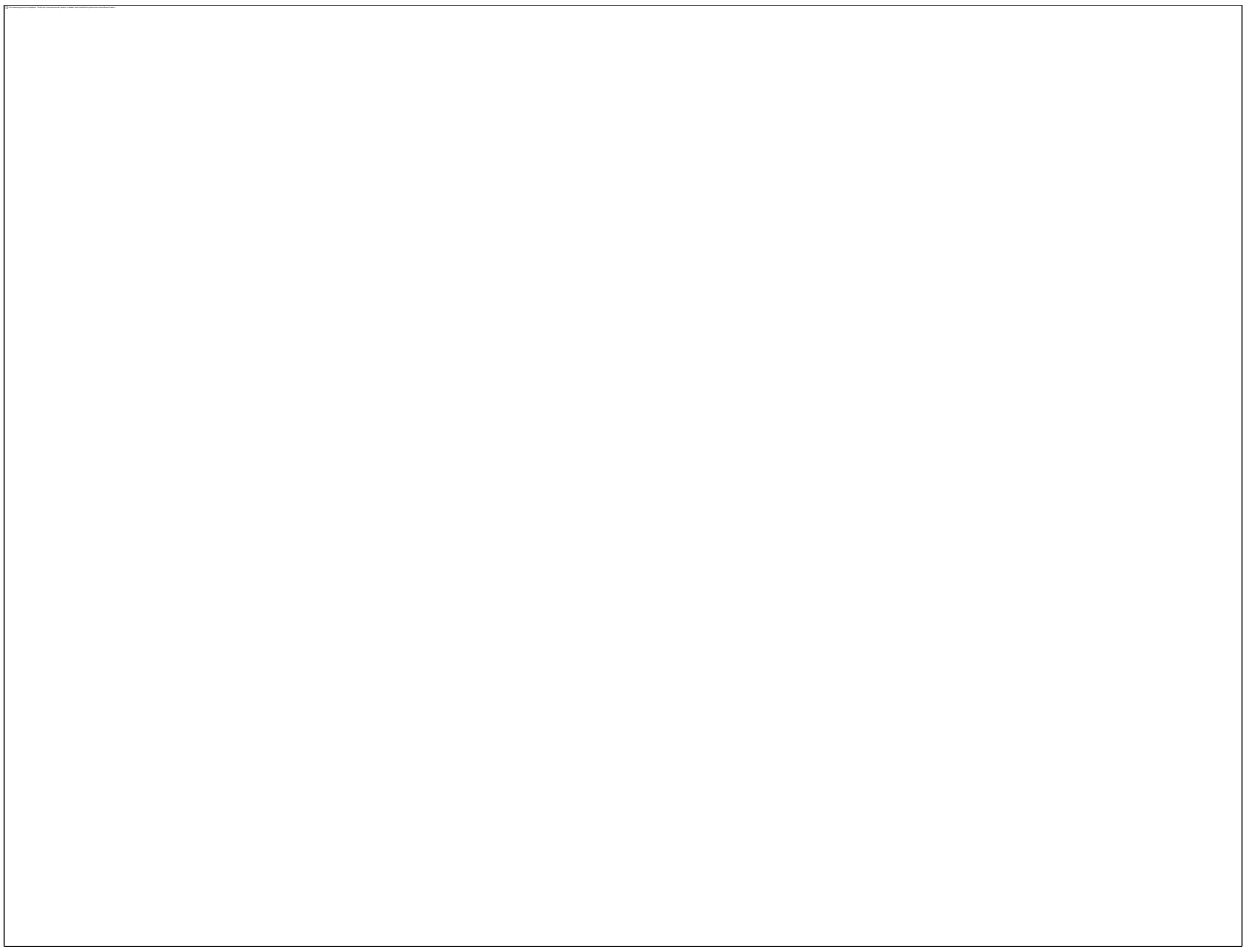

Figure 3 Summary data of duty cycle for Phr and XII with respect to temperature

Solid black circles represent data from the baseline condition; open circles are taken from the recovery period. The mean value and variability remains similar across temperatures studied.

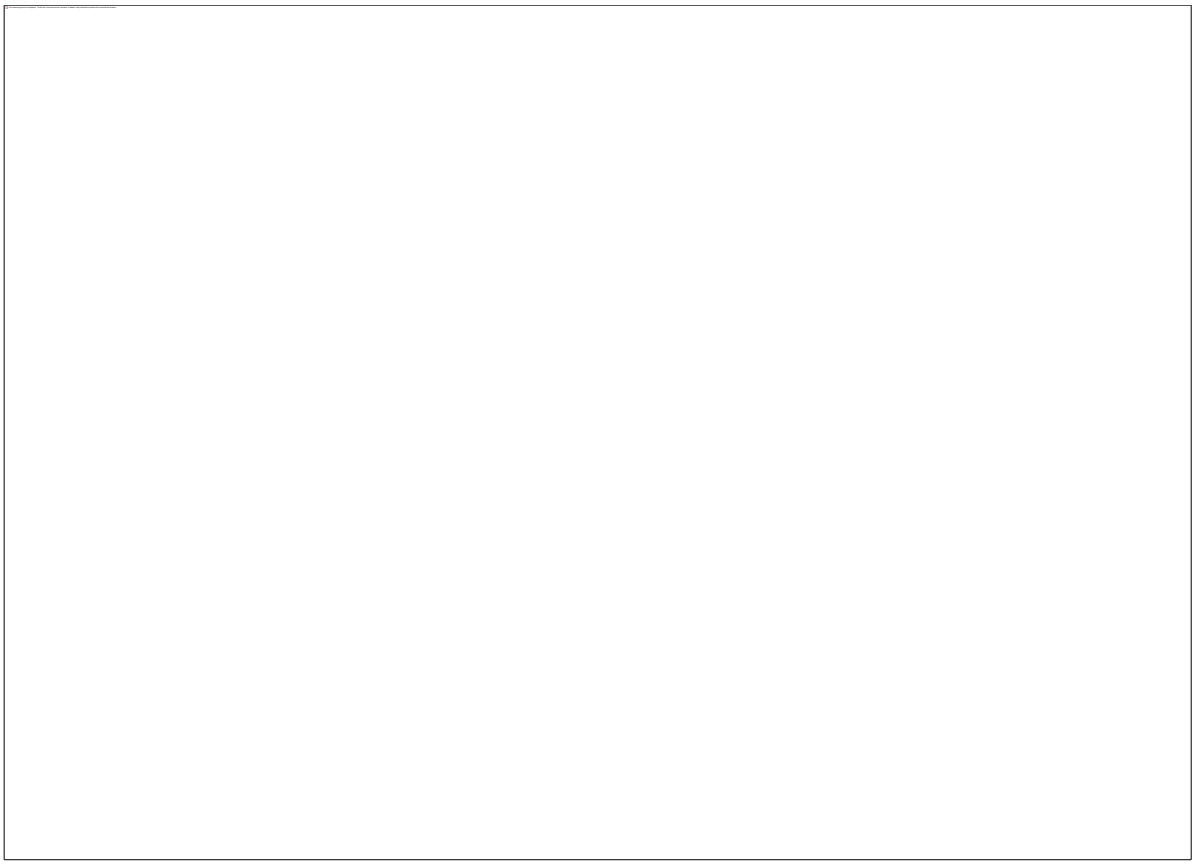

Figure 4 Phr and XII ApEn values with respect to temperature.

Individual and summary data from baseline, low temperature and high temperature conditions from experiments that had all 3 temperature groups. Yellow diamonds show the average of the phrenic data for a given temperature group; cyan diamonds show the average XII data for a given temperature group. Low temperature and basal temperature ApEn values of Phr nerve activity were significant compared to high temperature values for all 3 series of experiments. ApEn values between . ApEn values between Phr and XII data were significant in the low and baseline temperature groups. *$P<0.05$

Figure 5 The effect of temperature on power spectral density and spectral analysis characteristics.

Top left panel: Example normalized power spectral density plots from BL, LT and HT conditions from the same experiment. For these data all temperature groups were treated as independent groups. Blue denotes the low temperature group; black denotes baseline data; and red denotes the high temperature group. Top right panel: Summary data of the ratio of the power (amplitude) of the dominant MFO peak over the HFO peak. At lower temperatures, the MFO peak is the dominant peak, and at higher temperatures, the HFO peak becomes more dominant. Bottom panels: Summary data of the peak frequencies within the MFO and HFO ranges. HFO frequency increases linearly with respect to temperature at ~4.2Hz/˚C. * $P<0.05$

Figure 6 Example TF spectrum for different temperature groups from a single experiment

The temperature denotes the temperature of the cranial vault. Top panel: Original TF spectrum on their own relative scales (dark blue reflects 0 activity, and red reflects maximal activity (a.u.)). Bottom panel: TF spectrum normalized to the highest power across the entire experiment. TF spectral data confirms the patterns seen in time-invariant spectral analysis but shows that the timing of maximal activity changes as temperature changes; specifically, a majority of the dominant MFO and HFO activity appears earlier in the burst as temperature increases.

Figure 7 Composite TF spectrum in a contour plot from a single experiment

The dominant HFO activity changes in the same direction as the temperature. The power of MFO activity changes in value opposite of the direction of the temperature change. At the point of a temperature change, there is a large change in both MFO and HFO activity that recovers slightly as the cranial vault temperature stabilizes.

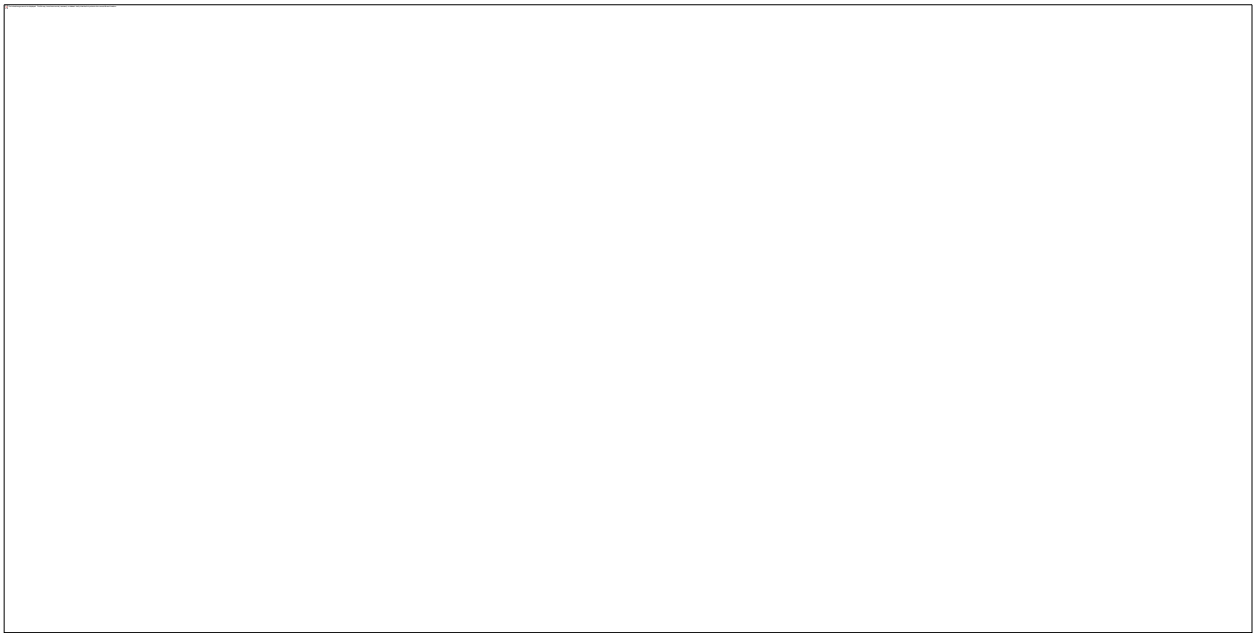

Figure 8 Example raw traces of integrated and raw phrenic and XII nerve output in response to extracellular changes in potassium.

Top panel: Example 30 second simultaneous recordings from both phrenic and XII nerve output from different experiments. The concentrations reported are that of the final K^+ concentration of the aCSF. f_b increases as$[K^+]_o$ increases, but the amplitude remained unchanged. Bottom panel: example bursts from each level of K^+. The burst shapes and timing relationships between the two nerves largely remains the same.

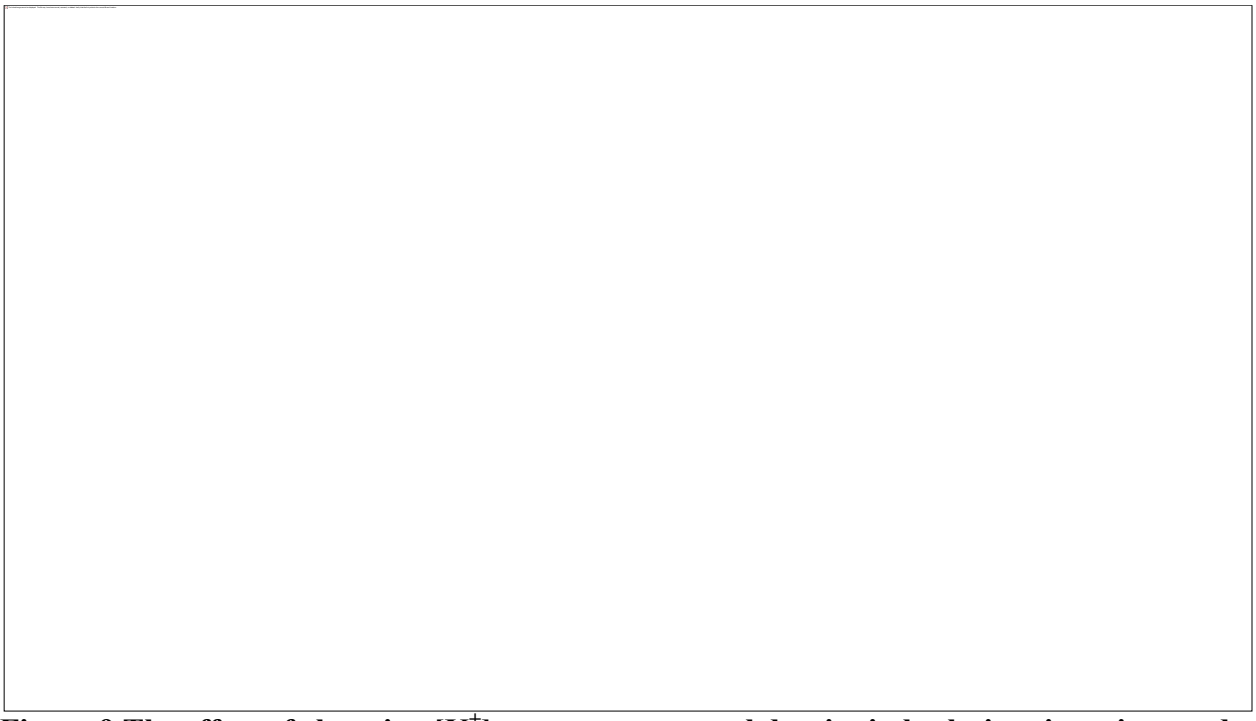

Figure 9 The effect of changing $[K^+]_o$ on power spectral density in both time-invariant and time-varying domains.

Left panel shows example spectral data from 1 experiment (3.0 mM baseline to 6.25 mM), and the right panel shows example spectral data from a different experiment (6.25 mM baseline to 9 mM). The top panels show the power spectral densities of both conditions overlaid with each other. No significant change due to K^+ variation detected in the frequencies of the MFO or HFO peaks or powers. The bottom panel are the respective TF plots normalized to the condition with the higher power. No significant change was seen in the timing of when peak activity occurred within the burst.

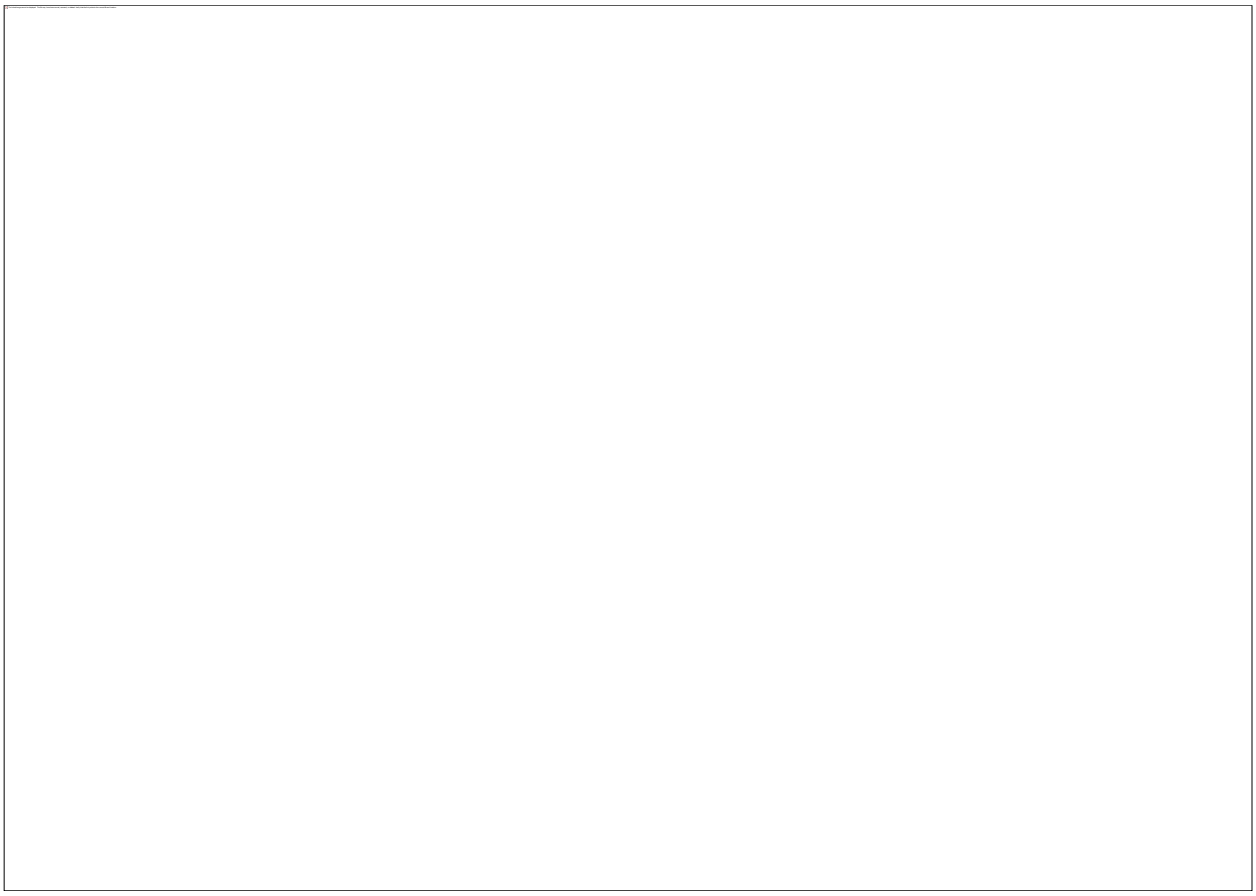

Figure 10 Comparison of inspiratory-phase complexity in Phr and XII at different levels of $[K^+]_o$

ApEn values for both Phr nerve output and the inspiratory portion of the simultaneously recorded XII nerve output. * denotes significant difference ($P<0.05$) between Phr and XII_I ApEn values. † denotes significance ($P<0.05$) between the two groups for Phr nerve output.

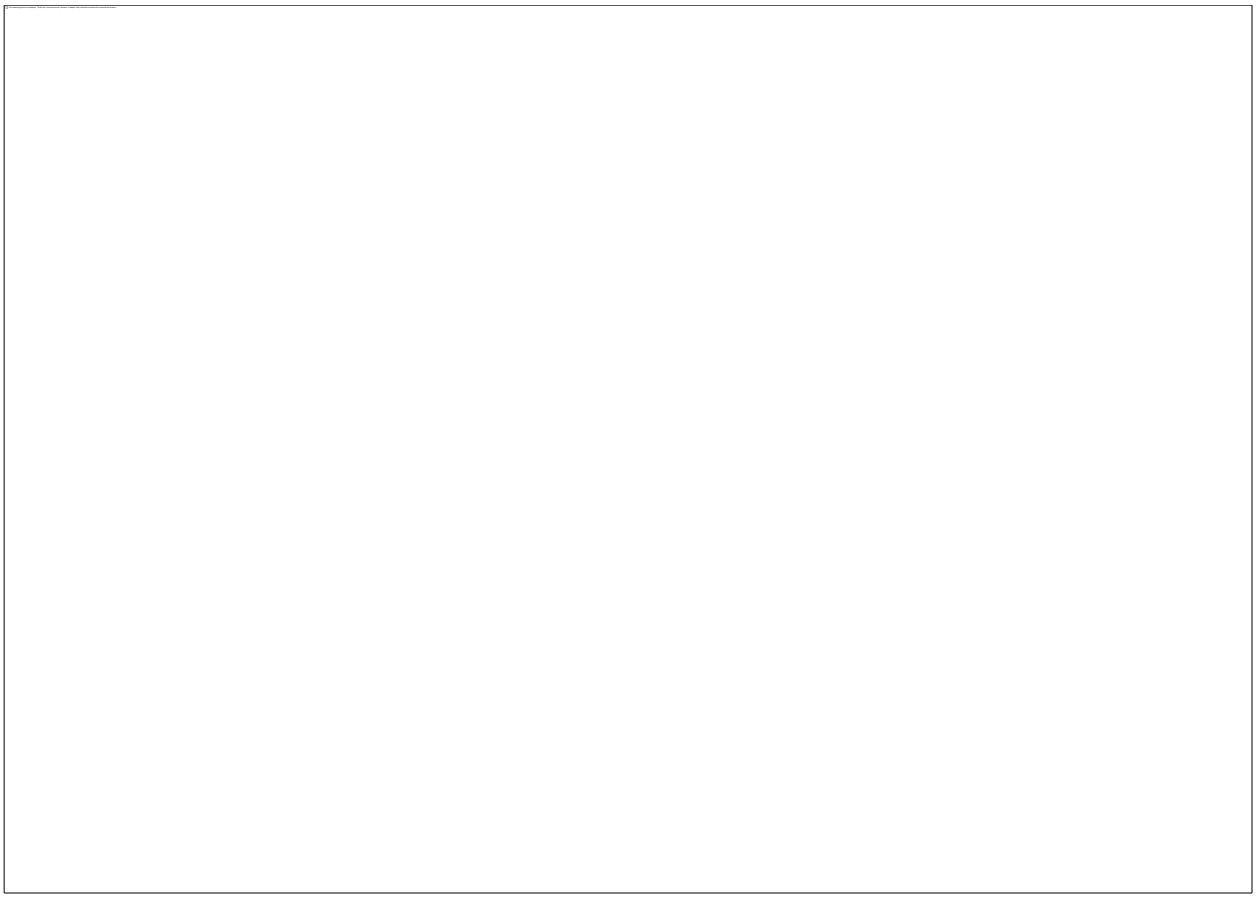

Figure 11 Comparisons of complexity in XII output phases at different levels of $[K^+]_o$

ApEn for XII_P, XII_I and XII_{P+I} nerve discharge. from series 1 experiments. * denotes significant difference between XII_P and other nerve phases ($P<0.001$)

Table 1 Summary temperature characteristics for the experimental groups

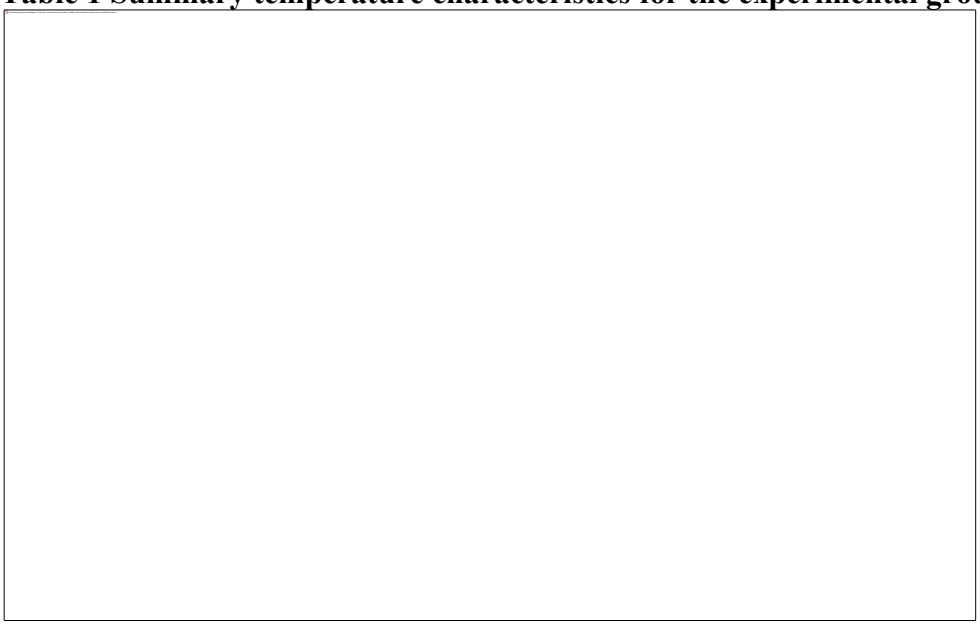

Table 2 Burst durations in ms

* denotes significant difference between PHR, XII_P and XII_{P+I} ($P<0.001$) at each level of $[K^+]_o$

† denotes significant difference between 3.0 and 9.0 mM and between 6.25 and 9.0 mM (P=0.010)

‡ denotes significant difference between 3.0 and 9.0 mM and between 6.25 and 9.0 mM (P=0.035)

Chapter 3: Functional Relationship between Respiration and the Micturition Reflex

Introduction

The respiratory system and micturition reflex both work to maintain homeostasis of very different physiological systems; the respiratory system is involved in maintaining blood gas homeostasis, and the micturition reflex is part of the system involved in maintaining water and ion homeostasis. While their functions and mechanics are vastly different, parts of their systems overlap in at least three areas: they are affected by overlapping neuromodulatory infleunces (e.g., 5-HT, dopamine), involve the use of abdominal muscle, and changes in abdominal pressure affect afferents in both the respiratory system and bladder stretch receptor feedback.

The micturition reflex consists of two main phases: storage (continence) and evacuation (voiding, micturition). Sympathetic stimulation maintains internal and external urethral sphincter tone and inhibits detrusor muscle contraction, allowing for urine storage. Sympathetic firing peaks during the guarding reflex, which occurs directly prior to active voiding. When bladder stretch reaches a threshold, ascending afferents pass through relay neurons in the periaqueductal grey (PAG), which is involved in the switch from storage to voiding (Blok, De Weerd, & Holstege, 1995; Fowler, Griffiths, & de Groat, 2008; Gert Holstege & Mouton, 2003), to the pontine micturition center. During voiding, parasympathetic tone to the via the pelvic nerve increases and sympathetic activity via the hypogastric nerve decreases which causes the internal sphincter to relax and the bladder to contract. In the rat, the external urethral sphincter bursts during active voiding.

Previous work has shown that there is some interaction between the respiratory system and micturition reflex. In cats, breathing frequency was modulated during a micturition event

(Sasaki, 1998), and the amplitude of phrenic and, more profoundly, hypoglossal nerve output decreased during micturition (Bartlett Jr & Knuth, 2003; Gdovin, Knuth, & Bartlett, 1994; Stella, Knuth, & Bartlett Jr, 2000). However, it is not clear how the level of respiratory drive may affect this functional interaction since blood gases and ventilation parameters were not reported. Some of our preliminary studies have indicated that micturition may have a greater effect on respiratory rhythm generation at or near apneic threshold, and it is unclear from previous studies whether or not the relationship between breathing and micturition changes as respiratory drive changes. Additionally, the relationship of respiratory drive on micturition has not been investigated. This study explores the effect of micturition and respiration, and the effect of respiratory drive on the micturition reflex. We hypothesize that there is a mutual interaction between the two systems, but that the interaction is subtle and may be more pronounced when respiratory drive is low.

Methods

Anesthesia

Adult female Sprague-Dawley rats (n=8 ; Taconic, Hudson, NY) were inducted with isoflurane (5%) and switched over to urethane to better control the depth of anesthesia. Urethane has been shown to be the most suitable anesthetic for acute studies of reflex micturition in rats (Matsuura & Downie, 2000), and has been used in the majority (>90%) of micturition studies in anesthetized rodents (for review, see (Andersson, Soler, & Füllhase, 2011)). Urethane also commonly is used in respiration-related studies. A total dose of 1.4 g/kg urethane was administered initially - 0.8 g/kg was administered sub-cutaneously just before surgery started, and 0.4 g/kg slowly was administered intravenously over a period of 2 minutes; 5 or 10% supplements were given i.v. as needed. Thereafter, the rat was weaned off of isoflurane over a period of 30 minutes. Recording began no sooner than 1 hour after the cessation of isoflurane

due to its reversible depressive effects on the micturition reflex(H.-Y. Chang & Havton, 2008; Leung, Johnson, & Wrathall, 2007; Smith, DeAngelis, & Kuchel, 2012).

Surgical Procedure and Animal maintenance

Animal vitals and physiological parameters (temperature, blood pressure, blood gasses and pH) were monitored and maintained close to physiological values throughout the experiment. Body temperature was monitored through a temperature probe inserted into an incision in the abdomen and maintained via a heat lamp and warm water bottles placed adjacent to the body. Blood pressure was monitored by a pressure gauge connected to a catheter inserted into the carotid artery. pH and blood gases were sampled from blood samples from the carotid artery and measured by a blood gas analyzer (ABL800 FLEX; Radiometer, Brønshøj, Denmark). To prevent metabolic acidosis, pH was maintained by an i.v. injection of $NaHCO_3$ (0.3cc of 8.4% NaHCO3 in saline) into the jugular vein as soon as the line was established. The animals were vagotomized, tracheostomized and mechanically ventilated to control blood gases. The animal was ventilated at about 36 breaths per minute with a gas mixture of 40% O_2, N_2 balanced.

The bladder was exposed through an abdominal incision and catheterized through the dome of the bladder (PE 90 tubing) to allow for controlled emptying and filling and was connected to a pressure gauge for intravesical pressure recording.

EMG activity from respiratory- and micturition-related muscles was recorded (Figure 12). Electrical signals were recorded from the diaphragm (Dia; upper right quadrant) and external urethral sphincter (EUS). EMG signals were also recorded from the styloglossus muscle in the tongue (T) and external oblique (EO) but are not shown in the presented data. Bipolar recordings using fine stainless steel wires inserted into the muscle were used for T, Dia and EO recordings, and the splayed tips of fine braided stainless-steel wires were placed on the

diaphragm for recordings. All data were recorded at 2k Hz; T, Dia and EO recordings were filtered by a 10 to 1kHz bandpass filter and EUS data were filtered by a 100-1kHz bandpass filter.

Experimental Protocol

Prior to recording the bladder was siphoned empty by opening the end of the catheter to the air and maintained empty while apneic threshold was being established. Animals were driven to apneic threshold, defined as the $PaCO_2$ where respiratory-related EMGs were silent for at least 4 minutes, by increasing the ventilator rate. Once apneic threshold was established, the ventilator rate was adjusted such that the $PaCO_2$ was 3 mmHg above apneic threshold. Thereafter, the bladder was filled with room temperature 0.09% saline at a constant rate (3-5 mL/hour) to produce micturition events no more frequently than every 2 minutes, although in 3 of the experiments the bladder was filled such that micturition events occurred as frequently as every 25 seconds. The recording protocol (Figure 13) comprised baseline data, a CO_2 challenge (7.2% CO_2, 40% O_2, N_2 balance) and a recovery (40% O_2, N_2 balance) period. Each condition was split into two parts (an early and a late period) by an arterial blood gas sample. The duration of each condition was determined by number of micturition events; each early and late period had at least 7 micturition events (~30 minutes).

Data Analysis and Statistical Tests

Bladder pressure and EUS data were downsampled to 100 Hz for analysis using IGOR Pro (Wavemetrics, Portland, OR) (Figure 14). Measurements from each micturition event included micturition threshold (the pressure at which the rate of pressure changed significantly), maximum and minimum bladder pressure, inter-contraction interval (the interval between micturition events), bladder contraction duration (the time between micturition threshold to the minimum bladder pressure) (Figure 15), EUS bursting duration, EUS burst event number and

frequency and EUS EMG area (i.e., integral of rectified EUS EMG activity) (Figure 16). The first micturition event after a change in gas mixture or arterial blood gas sampling was not included in analysis.

Breathing frequency was calculated in order to assess level of respiratory drive behaviorally. For baseline breathing, breathing frequency (f_b) was reported as the number of breaths of the last 2 minutes of the condition divided by the time. The average f_b for the CO_2 challenge and recovery periods were calculated as the number of breaths of about 2 minutes of data at the end of the early and late portion of their respective condition divided by the time.

To elucidate the effect of micturition on breathing frequency, histograms showing the initiation of breaths relative to activation of micturition were generated. The time of the initiation of breaths relative to the threshold for micturition were noted for a window of 30 seconds before and after the threshold. These data were binned into 5 second bins centered around 0 seconds (the time at which bladder pressure reached the micturition threshold), for a total of 13 bins. The first and last bins were discarded to avoid edge effects. To give an index of whether the number of breaths changed before and after micturition threshold, a ratio of the sum of breaths in bins 8-11 were divided by the sum of breaths in bins 3-6. Experiments where micturition frequency prevented binning breaths without overlap were excluded from these analysis.

A one-way repeated measures ANOVA was used to test for significance between conditions, and where appropriate a Holm-Sidak post-hoc was used ($\alpha = 0.05$). All values are expressed as mean±SE.

Results: Effects of micturition on breathing

As expected, the addition of CO_2 to the inspired gas mixture significantly increased breathing frequency (~31 to 44 bpm) and $PaCO_2$ (~35 to 64 mmHg) and significantly decreased

pH (~7.41 to 7.16) (Table 3). Because the ventilated gas mixture is controlled, it is unexpected that we saw an increase in PaO_2 (~197.6 to 227.6 mmHg), although the change is insignificant. The data indicate that the animal recovered fully after the long-duration CO_2 challenge. The increase in CO_2 did not change the basic characteristics of the micturition response; the 3 phases of micturition - guarding reflex, phasic active voiding and sustained relaxation - were present regardless of respiratory drive (Figure 17a). While subtle changes (e.g., there may be a trend of micturition duration increasing with increased respiratory drive) in the micturition reflex may be obscured by the large variability in the reflex (Figure 17b), the reflex is robust regardless of respiratory drive. In fact, in other experiments (data not shown) normal-looking micturition reflexes were observed even when the state of the rat was far outside physiological ranges.

At apneic threshold breathing was initiated once bladder filling resumed. In 5 rats, initiation of breathing corresponded to the onset of a micturition event (Figure 18a). However, micturition events were present prior first breathing efforts. Furthermore, once breathing was initiated it was not necessarily maintained (Figure 18b). In 3 of these 5 rats, breathing efforts did not return after bladder filling resumed; instead respiratory rhythm was initiated due to a ventilator frequency change and not micturition. In 2 experiments, the bladder filling rate was high and produced micturition events as frequently as every 25 seconds. These two experiments yielded variable respiratory rhythm onset markers; while some respiratory initiation was correlated with the onset of micturition, an equal amount was initiated between events, particularly when the timing between the events were short. In 1 experiment, breathing was initiated prior to a productive micturition event, although rapid non-voiding micturition events were present, and respiration ceased at micturition event (Figure 18c)

Figure 19a is an example histogram of initiation of breaths with respect to the threshold point of micturition during the CO_2 challenge and recovery period overlain with a line-graph representation of the histogram under baseline condition. During baseline conditions, there is a difference in breathing frequency before and after the initiation of micturition that is not present during addition of CO_2 and during the early recovery period, but does return during the late recovery period. Summary histograms of 5 experiments are shown in Figure 19b, which shows the relative change in frequency by reporting the ratio of number of breaths after an initiation of micturition over the number of breaths before the initiation of micturition. Experiments where micturition frequency prevented binning breaths without overlap were not included. The large magnitude of the standard error in the baseline and Rec_L conditions probably reflects an effect of the animal being near the apneic threshold.

Discussion: Effects of micturition on breathing

In the present study, we explored the effects of the micturition reflex on breathing at different levels of respiratory drive. We hypothesized that the contribution of micturition on breathing would diminish as respiratory drive increased. Our results support this hypothesis: at low levels of respiratory drive (at or near apneic threshold) bladder contractions mostly provided an excitatory effect on the respiratory system, manifested primarily as an increase in breathing frequency, but also in the initiation of breathing. At higher levels of respiratory drive, the effects of bladder contractions on breathing were undetectable.

Data exploring the relationship between central reflex pathways to the lower urinary tract and breathing has been studied primarily in the decerebrate cat. Due to the shift in literature toward rodent models in both respiratory and micturition fields, we thought it necessary to explore whether the relationship was species specific. Our results confirm the findings presented

in the only study on this reflex in rats. Stella et al.(Stella et al., 2000) reported that, unlike decerebrate cats, micturition reflexes in artificially-ventilated decerebrate rats were not associated with a decrease and amplitude of phrenic and XII nerve output. This study, however, did not look at transient changes in breathing frequency. We observed a mostly excitatory change in frequency associated with a micturition reflex, but only at or near apneic threshold, which also can be seen in phase II of the micturition events in the Stella et al. study, indicating that it is not an effect of anesthesia.

While SBCs contain a high degree of variability, they showed the same characteristic pattern irrespective of the change in CO_2, and they appear to be similar qualitatively to micturition events in decerebrate rats. Subtle changes seem to exist, but they were not large enough to be significant or perhaps our characterization measures were not sensitive enough to detect these changes. We do not believe that the subtleties are a consequence of anesthesia, because urethane has a low depressive effect on cardiorespiratory systems, and does not seem to affect micturition events when compared to decerebrate rats (Yoshiyama, Roppolo, Takeda, & de Groat, 2013).

The loss of breathing frequency change due to micturition (Figure 19) under higher respiratory drive leads us to believe that the balance between LUT and respiratory feedback tipped such that the LUT contribution to respiratory modulation is weaker at high respiratory drive. Resolution of the histograms due to the increase in f_b as a result of added CO_2 to the inhaled gas mixture was not a contributor to these conclusions; even at finer resolutions (as low as 2 second bin sizes) the pattern was conserved. Additionally, the large variability in baseline and Rec_L period suggests that the contribution of micturition on the variability of f_b is highly dependent on how close to apneic threshold we were. Establishing apneic threshold, and

therefore a consistent baseline, while the bladder was distended or filling proved to be a challenge. While apneic periods would appear, we observed that the apneic threshold while the bladder was filling was lower than apneic threshold while the bladder was empty. We also observed that hysteresis was larger during a filled or filling bladder when attempting to bring the $PaCO_2$ to 2-3 mmHg. These observations also support the idea that LUT activity has a role in respiratory excitability at apneic threshold.

These results suggest that an excitatory link exists between the neural circuits that control micturition and breathing, however, the mechanism for this excitatory link cannot be elucidated from this study. One possible explanation is that sensory pathways from the bladder converge and directly modulate respiratory rhythm (G Holstege, 2013). If so, the likely point of convergence is the periaqueductal grey (PAG), since neural circuits involved in both breathing and the micturition reflex have synapses there (G Holstege, 2013; Gert Holstege & Mouton, 2003): the PAG has been shown to be a key area in converting basic breathing to behavioral breathing (Subramanian, 2013; Subramanian, Balnave, & Holstege, 2008; Subramanian & Holstege, 2010) and stimulation of the PAG has been shown to modulate preinspiratory neurons in the pre-Bötzinger complex by changing firing rate and altering the respiratory phases when these neurons fire (Subramanian and Hostege 2013); the bladder projects afferent sensory information to the PAG, which is thought to be the area of the brain responsible for activating the pontine micturition center, thereby switching from continence to active sustained contraction (Fowler et al., 2008). However, activation of areas in the PAG still could affect breathing indirectly through its strong projections to the nucleus retroambiguus (G Holstege, 2013). A second possible explanation for the two systems interact indirectly could be a result of the strong parasympathetic nervous system activation during the switch from continence to micturition

activates neuromodulatory systems (e.g., serotonin, dopamine), which then has an effect on breathing. A third possible explanation is the recruitment of abdominal muscles during active expiration. EO muscles, normally quiescent during eupnea and recruited during micturition (H. H. Chang & Havton, 2012; Cruz & Downie, 2006), are recruited strongly during active expiration, and large abdominal movements can be observed clearly. While the muscles may be recruited, abdominal pressure change due to these movements can be ruled out as an explanation due to the large opening in the abdomen to the atmosphere.

It may be advantageous that there is a shift such that micturition contributes to respiration less as respiratory drive increases. In instances where respiratory drive is elevated due to a gas exchange imbalance (e.g., exercise or pulmonary disease), the necessity for micturition becomes much less important with respect to survivability.

Results: Effects of respiratory drive on micturition

Data collected from bladder pressure measurements included the contraction duration, threshold pressure, peak pressure and the time between micturition events (intercontraction interval (ICI)). The averages of each of these parameters were calculated and the results were summarized in Table 3. Figure 20 shows the ratio of change for parameters associated with bladder pressure. Compared to baseline, the addition of CO_2 significantly increased the bladder threshold pressure. This change in threshold recovered when CO_2 was removed, but there was a delay to full recovery and the parameter did not recover fully until the Rec_L period. This suggests that prolonged increases in respiratory drive raises the bladder volume/threshold needed to elicit a micturition event. Contraction duration may increase then recover due to the CO_2 challenge, but due to large variability, these changes were not significant. Both a significant increase in minimum bladder pressure between baseline and the Rec_E period and a large difference in

variability between the CO_2 challenge and recovery were observed. Peak bladder pressure was unaffected by the CO_2 challenge, and the inter-contraction interval (ICI) varied greatly and resulted in no significant change as a result of the CO_2 challenge.

Measurements collected from EUS EMG signals normalized to their baselines are shown in Figure 21. These measurements include burst duration, number of bursts, burst frequency and area under the EUS EMG (an index of sustained EUS activity). During the CO_2 challenge, mean EUS bursting duration increased (2.00 to 2.64 s) and the number of EUS burst events decreased (14.5 to 13.1), although these changes were not statistically significant. EMG burst area decreased (2873 $\rightarrow$ 2429 μV*s) during elevated respiratory drive and recovered after some time, but the decrease was not significant. Burst frequency, however, decreased significantly during the CO_2 challenge (7.22 Hz (BL) to 5.33 Hz (CO_{2E})) and returned to baseline levels during the recovery period.

Discussion: Effects of respiratory drive on micturition

In the present study, we explored the effects of respiratory drive on the micturition reflex. We hypothesized that respiratory drive would have very little effect on the overall micturition reflex but may affect the timing of some of the phases. Overall, this study shows that the micturition reflex is very robust, but a prolonged increase in respiratory drive by CO_2 does changes characteristics of the micturition reflex, namely an increase in bladder threshold pressure and EUS bursting frequency.

Because respiratory drive was increased by hypercapnia, there are at least 4 mechanisms by which the increase in respiratory drive could affect micturition in the present study. First, elevated CO_2 could have a direct effect on the neural control of micturition. For example,

elevated CO_2 could decrease the sensitivity of neurons in or near the PAG or PMC producing an increase in micturition threshold (Coates, Li, & Nattie, 1993). Second, it is possible that hypercapnia could have an influence on bladder wall mechanoreceptors. CO_2 may have affected the bladder wall directly by inhibiting slowly adapting stretch receptors (Bartlett Jr & Sant'Ambrogio, 1976; Coates et al., 1993; Fedde, Kuhlmann, & Scheid, 1977; Mustafa & Purves, 1972), or it may have acted on the detrusor muscle directly, since hypercapnia has been shown to slightly increase the force of contraction in isolated strips of detrusor muscles (Liston, Palfrey, Raimbach, & Fry, 1991) while unaffecting peak bladder pressures (Bartlett Jr & Knuth, 2003) which is consistent with our data. A third, and most likely possibility, is that increasing respiratory drive activates neuromodulatory systems (e.g., serotonin, dopamine, norepinephrine) that alter the neural control of LUT function. Additional studies are needed to differentiate between these possible mechanisms. A fourth possibility is that the recruitment of abdominal muscles during increased respiratory drive may have activated mechanoreceptors in the bladder wall due to the movement or changes in pressure in the abdominal cavity. However, due to the large opening in the abdomen, this is not a likely contributor in this study.

Changing respiratory drive may have had an impact on voiding efficiency. Given the observed increase in bladder threshold pressure, one would expect that ICI should increase due to a delay in the transition from continence to incontinence; however, we did not observe this. Instead, we noted that ICI varied considerably throughout the experiments regardless of respiratory drive, and no significant increase was detected. It is possible that the ICI did not increase due to an increase in the minimum bladder pressure between micturition events. While an increase in minimum bladder pressure normally would indicate that the void was less efficient since the residual volume is greater, speculation on voiding efficiency is obscured by the

increase in threshold pressure. Changing respiratory drive had no significant effect on peak pressure during bladder contraction. However, the possibility of a ceiling effect cannot be ruled out. The contraction duration appeared to increase with the change in respiratory drive, although, due to the large degree of variability, the change was not significant. The decrease in EUS burst frequency also may indicate that voiding efficiency changed.

The increase in respiratory drive likely has an effect on the micturition central pattern generator (CPG). EUS burst frequency consistently and significantly decreased during hypercapnia. Previous studies indicate that EUS bursting is due to activation of a central pattern generator in the rostral lumbar spinal cord (L2-3) (H.-Y. Chang, Cheng, Chen, & de Groat, 2007; Dolber et al., 2007). Therefore, it is likely that increased respiratory drive has an effect on this EUS bursting CPG. With respect to voiding efficiency, frequency alone cannot determine whether there was a change in voiding efficiency; if the decrease in bursting frequency is accompanied by an increase in activation time (i.e., the duration of individual bursts are longer), then void volume could be reduced; however, if the duration of individual bursts were unchanged or shorter, then void volume could increase. Because data were not analyzed in such a way, and because the volume of each void was not measured, further analysis and data collection would be required in order to determine whether voiding efficiency was altered.

Conclusion

The respiratory system is a highly dynamic system, and the micturition reflex is a highly robust reflex. The two systems share anatomy and are functionally connected, and there seems to be a very subtle interplay between the micturition and respiratory system, which is more apparent at the ends of the spectrum.

Andersson, K. E., Soler, R., & Füllhase, C. (2011). Rodent models for urodynamic investigation. *Neurourology and urodynamics, 30*(5), 636-646.

Bartlett Jr, D., & Knuth, S. (2003). Influence of hypercapnia and hypocapnia on bladder contractions and their respiratory consequences. *Respiratory physiology & neurobiology, 134*(3), 247-253.

Bartlett Jr, D., & Sant'Ambrogio, G. (1976). Effects of local and systemic hypercapnia on the discharge of stretch receptors in the airways of the dog. *Respiration physiology, 26*(1), 91-99.

Blok, B. F., De Weerd, H., & Holstege, G. (1995). Ultrastructural evidence for a paucity of projections from the lumbosacral cord to the pontine micturition center or M-region in the cat: A new concept for the organization of the micturition reflex with the periaqueductal gray as central relay. *Journal of Comparative Neurology, 359*(2), 300-309.

Chang, H.-Y., Cheng, C.-L., Chen, J.-J. J., & de Groat, W. C. (2007). Serotonergic drugs and spinal cord transections indicate that different spinal circuits are involved in external urethral sphincter activity in rats. *Am J Physiol Renal Physiol, 292*(3), F1044.

Chang, H.-Y., & Havton, L. A. (2008). Differential effects of urethane and isoflurane on external urethral sphincter electromyography and cystometry in rats. *American Journal of Physiology-Renal Physiology, 295*(4), F1248.

Chang, H. H., & Havton, L. A. (2012). Modulation of the visceromotor reflex by a lumbosacral ventral root avulsion injury and repair in rats. *American Journal of Physiology-Renal Physiology, 303*(5), F641.

Coates, E., Li, A., & Nattie, E. E. (1993). Widespread sites of brain stem ventilatory chemoreceptors. *Journal of Applied Physiology, 75*, 5-5.

Cruz, Y., & Downie, J. W. (2006). Abdominal muscle activity during voiding in female rats with normal or irritated bladder. *American Journal of Physiology-Regulatory, Integrative and Comparative Physiology, 290*(5), R1436-R1445.

Dolber, P. C., Gu, B., Zhang, X., Fraser, M. O., Thor, K. B., & Reiter, J. P. (2007). Activation of the external urethral sphincter central pattern generator by a 5-HT1A receptor agonist in rats with chronic spinal cord injury. *American Journal of Physiology-Regulatory, Integrative and Comparative Physiology, 292*(4), R1699-R1706.

Fedde, M. R., Kuhlmann, W., & Scheid, P. (1977). Intrapulmonary receptors in the tegu lizard: I. Sensitivity to CO< sub> 2</sub>. *Respiration physiology, 29*(1), 35-48.

Fowler, C. J., Griffiths, D., & de Groat, W. C. (2008). The neural control of micturition. *Nature Reviews Neuroscience, 9*(6), 453-466.

Gdovin, M., Knuth, S., & Bartlett, D. (1994). Respiratory motor nerve activities during spontaneous bladder contractions. *Journal of Applied Physiology, 77*(3), 1349-1354.

Holstege, G. (2013). The periaqueductal gray controls brainstem emotional motor systems including respiration. *Progress in brain research, 209*, 379-405.

Holstege, G., & Mouton, L. J. (2003). Central nervous system control of micturition. *International review of neurobiology*, 123-147.

Leung, P. Y., Johnson, C. S., & Wrathall, J. R. (2007). Comparison of the effects of complete and incomplete spinal cord injury on lower urinary tract function as evaluated in unanesthetized rats. *Experimental neurology, 208*(1), 80-91.

Liston, T., Palfrey, E., Raimbach, S., & Fry, C. (1991). The effects of pH changes on human and ferret detrusor muscle function. *The Journal of physiology, 432*(1), 1-21.
Matsuura, S., & Downie, J. (2000). Effect of anesthetics on reflex micturition in the chronic cannula-implanted rat. *Neurourology and urodynamics, 19*(1), 87-99.
Mustafa, M., & Purves, M. (1972). The effect of CO< sub> 2</sub> upon discharge from slowly adapting stretch receptors in the lungs of rabbits. *Respiration physiology, 16*(2), 197-212.
Sasaki, M. (1998). Bladder motility and efferent nerve activity during isotonic and isovolumic recording in the cat. *The Journal of physiology, 510*(1), 297-308.
Smith, P. P., DeAngelis, A. M., & Kuchel, G. A. (2012). Evidence of central modulation of bladder compliance during filling phase. *Neurourology and urodynamics, 31*(1), 30-35.
Stella, M., Knuth, S., & Bartlett Jr, D. (2000). Respiratory response to spontaneous contractions of the urinary bladder in awake and decerebrate rats. *Respiration physiology, 120*(2), 105-114.
Subramanian, H. H. (2013). Descending control of the respiratory neuronal network by the midbrain periaqueductal grey in the rat in vivo. *The Journal of physiology, 591*(1), 109-122.
Subramanian, H. H., Balnave, R. J., & Holstege, G. (2008). The midbrain periaqueductal gray control of respiration. *The Journal of Neuroscience, 28*(47), 12274-12283.
Subramanian, H. H., & Holstege, G. (2010). Periaqueductal gray control of breathing *New Frontiers in Respiratory Control* (pp. 353-358): Springer.
Yoshiyama, M., Roppolo, J. R., Takeda, M., & de Groat, W. C. (2013). Effects of urethane on reflex activity of lower urinary tract in decerebrate unanesthetized rats. *Am J Physiol Renal Physiol, 304*(4), F390-396. doi: 10.1152/ajprenal.00574.2012

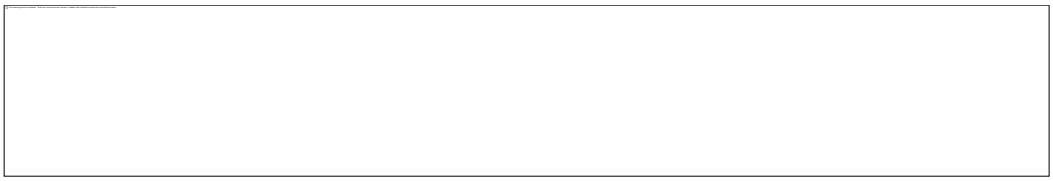

Figure 12 Recording protocol.

Baseline condition was 2-3 mmHg above apneic threshold with the bladder filled at a constant rate. CO_{2E} and CO_{2L}: Early and late portion of the CO_2 challenge, respectively. Rec_E and Rec_L: Early and late portion of the recovery period, respectively. ABG: arterial blood gas.

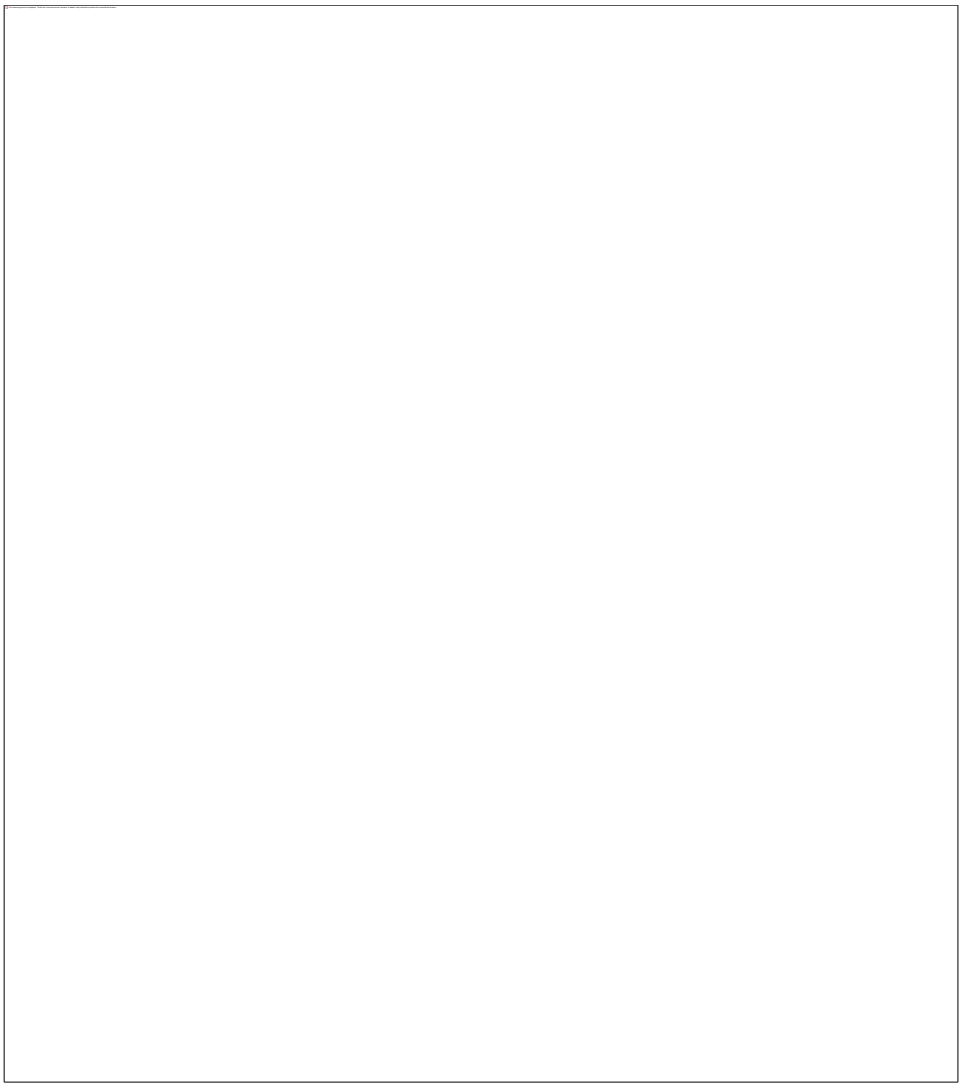

Figure 13 Experimental EMG recording setup.

Schematic showing EMG recordings. It should be noted that a large incision wad made in the abdomen and left open to record diaphragm EMGs. In most experiments femoral lines were used, but in o

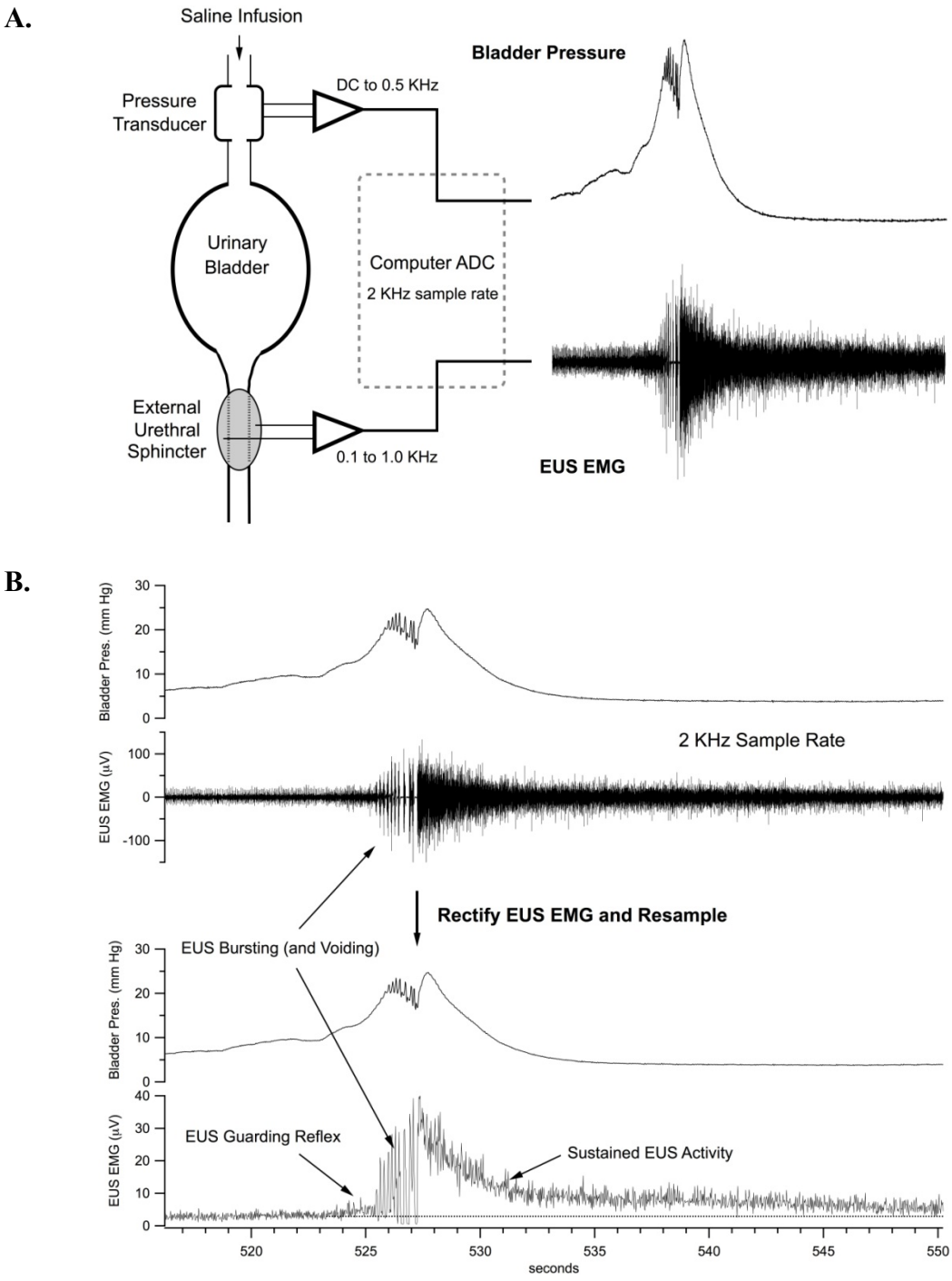

Figure 14 Bladder and EUS data recording schematic and data analysis pre-processing steps.

A: Illustration of simultaneous cystometry and EUS EMG recording during a micturition event elicited by infusion of saline (4.0-5.2 ml/hr) into the dome of the bladder. B: Records were rectified and resampled prior to making measurements.

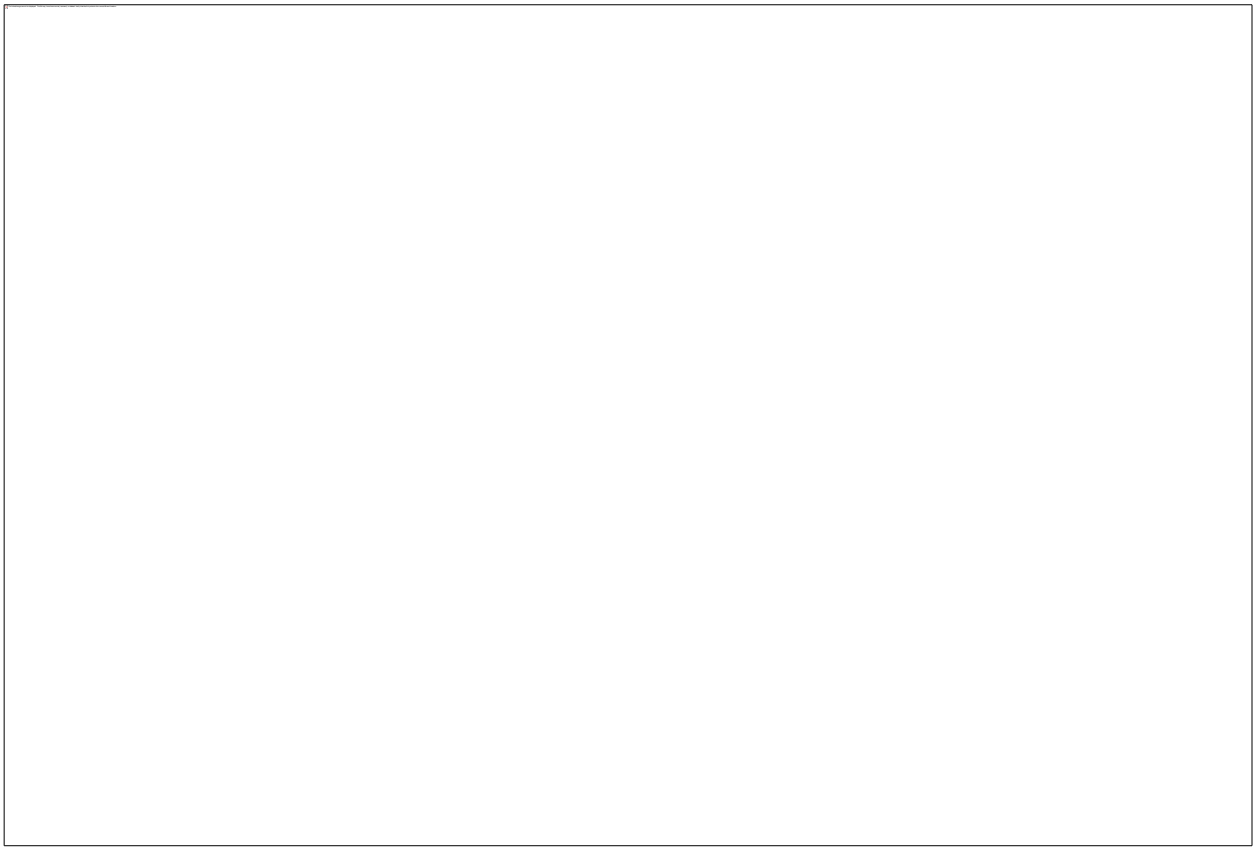

Figure 15 Quantification of bladder pressure during a micturition event.

Sample bladder pressure trace during a micturition event denoting points of analysis to characterize and measure a micturition event.

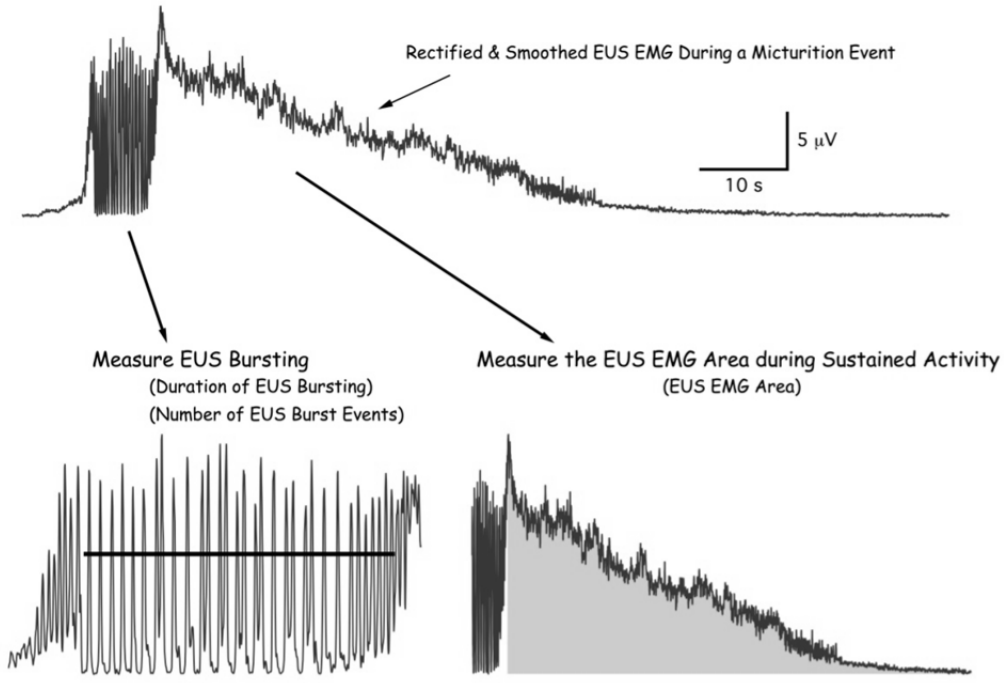

Figure 16 Quantification of EUS activity during a micturition event.

Sample integrated EUS trace during a micturition event denoting points of analysis to characterize and measure a micturition event.

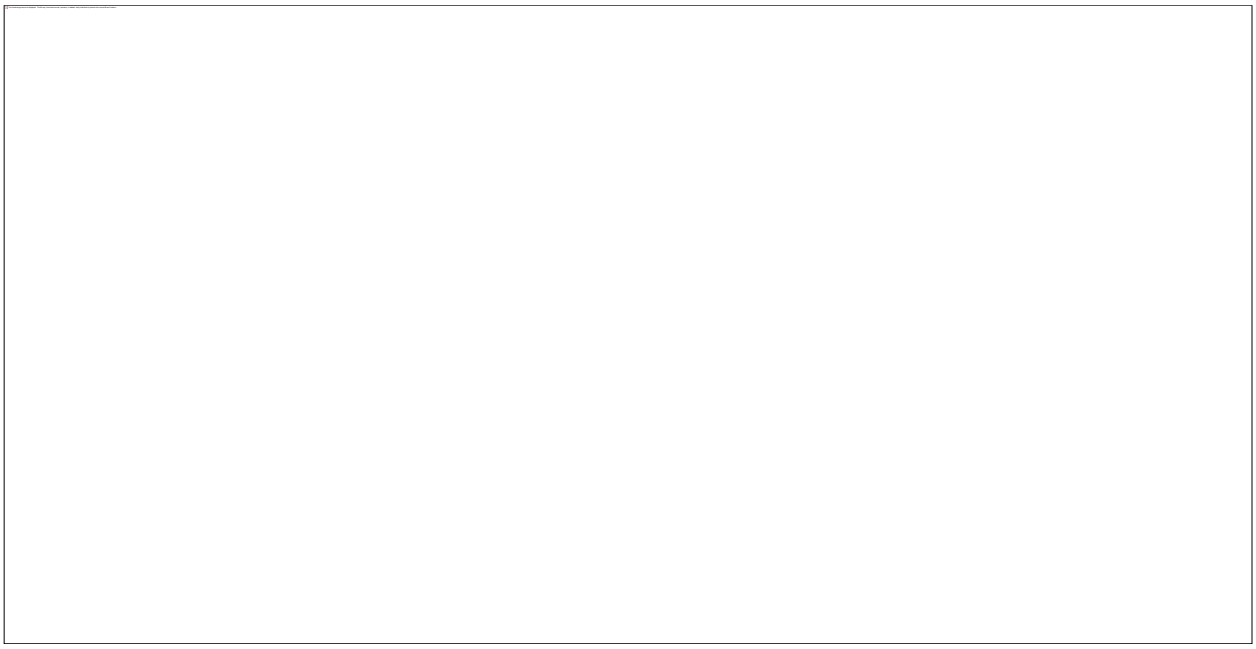

Figure 13 Micturition reflex is robust regardless of level of respiratory drive.

Panel A: sample bladder pressure traces from each respiratory drive condition. Panel B: Quantification of bladder pressure values.

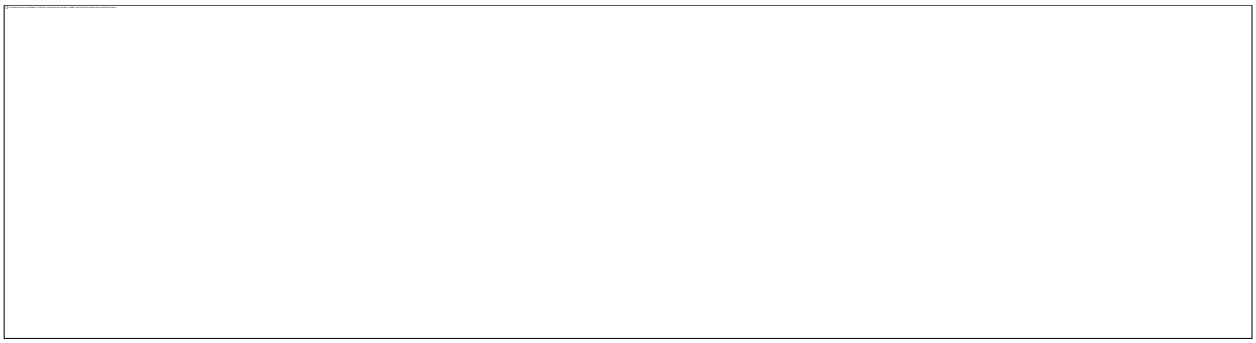

Figure 14 Micturition events alter respiratory drive at apneic threshold.

In most cases, at apneic threshold, the onset of respiration correlated with a micturition event (Examples A and B) and subsequent respiratory behavior may continue or may have short apneic periods. In 1 case the onset of respiratory behavior was not correlated with a micturition event (Example C), and instead the start of a long apneic period was initiated at a micturition event. It should be noted that the rate of bladder filling is much higher for Example C, which may be a contributing factor for the anomaly.

Figure 15 Representative histograms and summary relative f_b change data.

Panel A: Representative histograms for the experimental conditions overlaid with baseline histogram data, shown as a line-graph). Panel B: Summary data (n=5) showing the relative change in f_b over the experimental conditions. At baseline and Rec_L conditions there is an increase in respiratory frequency after a micturition event initiation that is not present during the CO_2 challenge. Data also shows the system requires some time to recover after such a long perturbation.

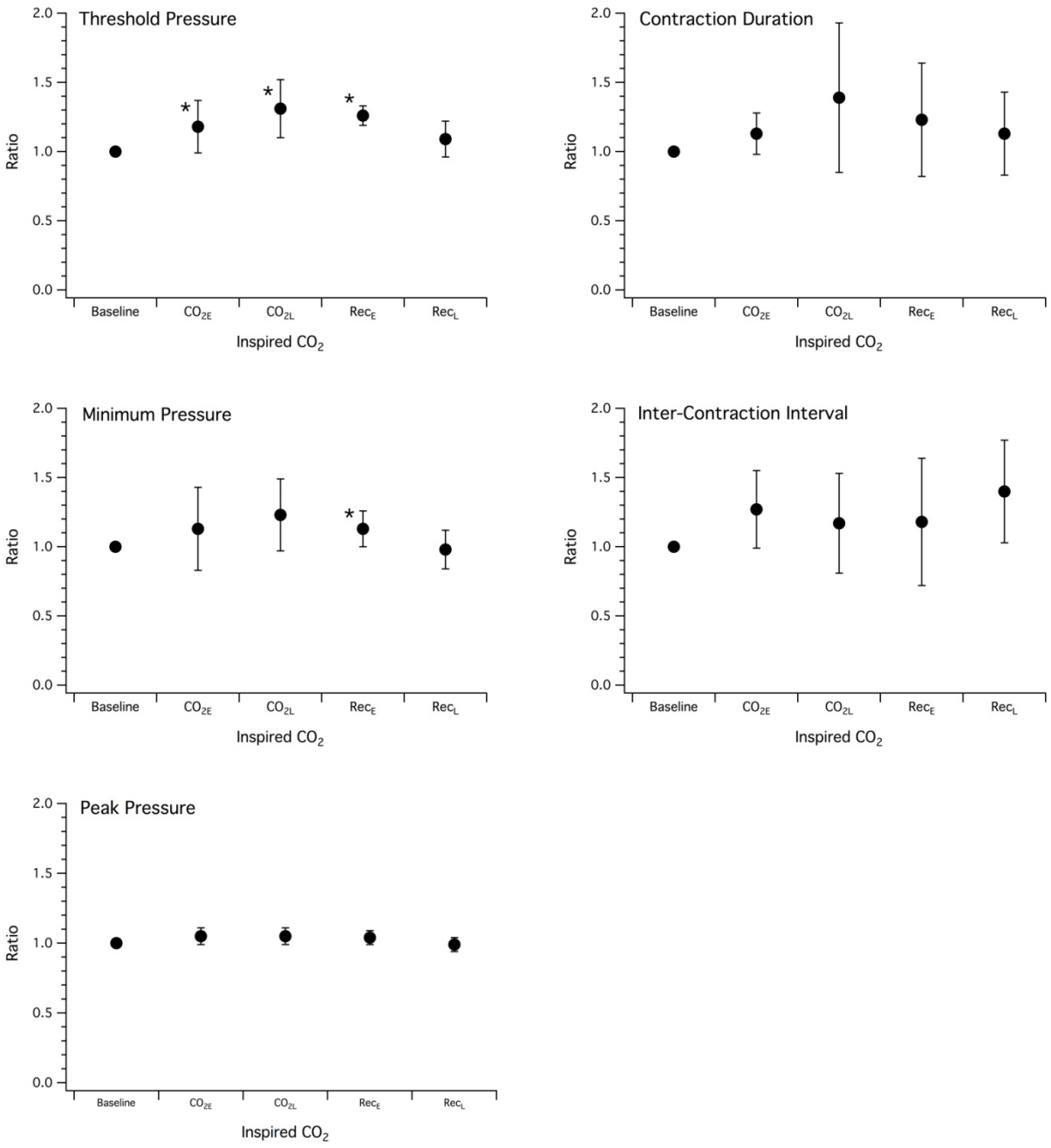

Figure 16. Summary data for characteristic bladder measurements during micturition.

Normalized means ± standard deviations of bladder threshold pressure, contraction duration, peak pressure, minimum pressure, and inter-contraction interval at different levels of inspired CO_2. Means normalized to 0% inspired CO_2 baseline (0% (pre)) for each rat (n=7). * indicates significant difference compared to 0% (pre) ($P<0.05$).

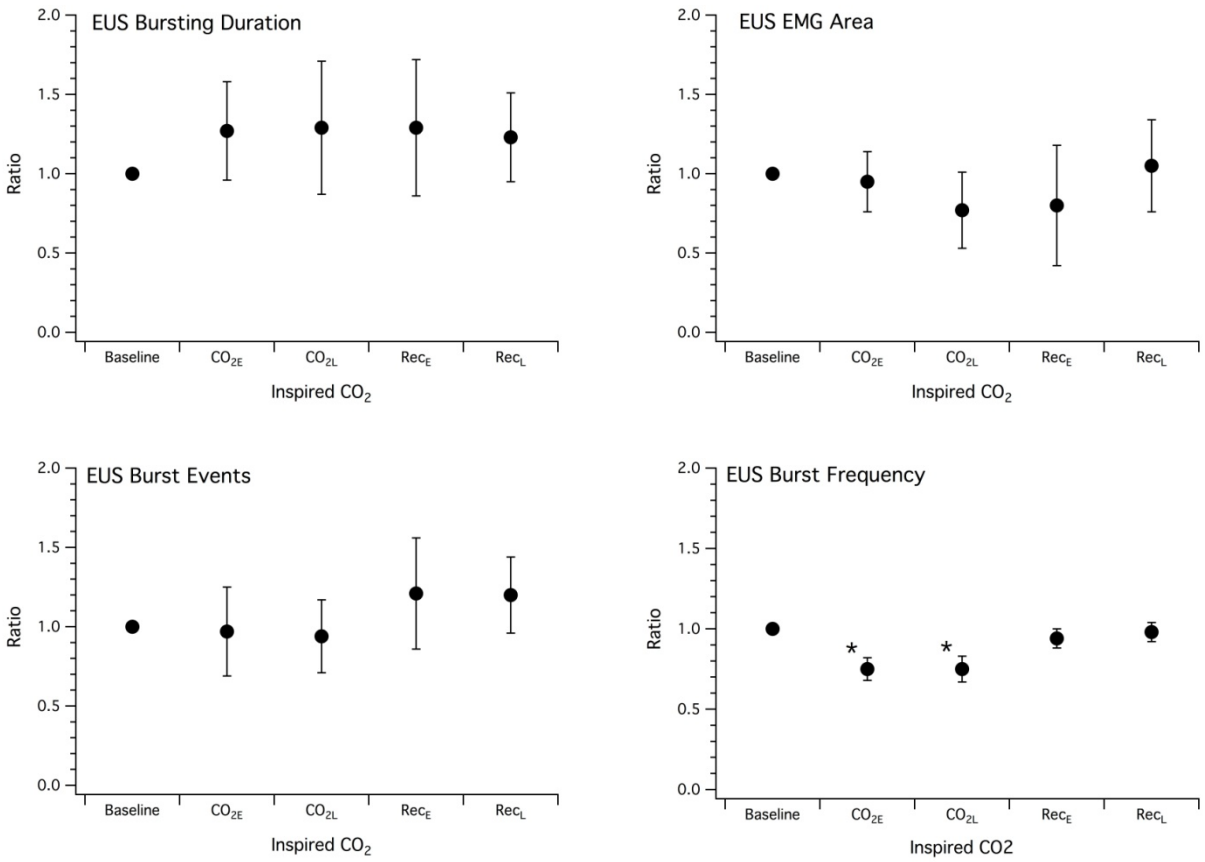

Figure 17. Summary data for characteristic bladder measurements during micturition.

Normalized means ± standard deviations of EUS bursting duration, burst event number, burst frequency, and EMG area at different levels of inspired CO_2. Means normalized to 0% inspired CO_2 baseline (0% (pre)) for each rat (n=5). * indicates significant difference compared to 0% (pre) ($\rho<0.05$).

Table 3 Table showing vitals monitoring.

Breathing frequency (f_b) and amplitude (not shown) increased significantly ($P<0.01$) during the CO_2 challenge. The significant change in $PaCO_2$ caused an acute respiratory acidosis as expected.